USE OF BODY COMPOSITION IMAGING TO CALCULATE 3D INERTIAL PARAMETERS FOR INVERSE DYNAMIC ANALYSIS OF YOUTH PITCHING ARM KINETICS

A Thesis

presented to

the Faculty of California Polytechnic State University,

San Luis Obispo

In Partial Fulfillment

of the Requirements for the Degree

Master of Science in Biomedical Engineering

by

Dalton Jennings

March 2020

COMMITTEE MEMBERSHIP

TITLE:	Use of Body Composition Imaging to Calculate 3D Inertial Parameters for Inverse Dynamic Analysis Of Youth Pitching Arm Kinetics
AUTHOR:	Dalton Jennings
DATE SUBMITTED:	March 2020
COMMITTEE CHAIR:	Stephen Klisch, Ph.D. Professor of Mechanical Engineering
COMMITTEE MEMBER:	Scott Hazelwood, Ph.D. Professor of Biomedical Engineering
COMMITTEE MEMBER:	Scott Reaves, Ph.D. Professor of Food Science and Nutrition

ABSTRACT

Use Of Body Composition Imaging To Calculate 3-D Inertial Parameters For Inverse Dynamic Analysis Of Youth Pitching Arm Kinetics

Dalton J. Jennings

The objectives of this study were to 1) calculate participant-specific segment inertial parameters using dual energy X-ray absorptiometry (DXA) data (referred to as full DXA-driven parameters) and compare the pitching arm kinetic predictions using full DXA-driven inverse dynamics vs scaled, DXA mass-driven (using DXA masses but scaled centers of mass and radii of gyration), and DXA scaled inverse dynamics(ID) (using the full DXA-driven inertial parameters averaged across all participants), 2) examine associations between full DXA-driven kinetics and body mass index (BMI) and 3) examine associations between full DXA-driven kinetics and segment mass index (SMI). Eighteen 10- to 11- year-olds pitched 10 fastballs. DXA scans were conducted and examined to obtain 3D inertial parameters of the upper arm, forearm, and hand. Full DXA-driven and scaled inertial parameters were compared using paired t-tests. Pitching arm kinetic predictions calculated with the four methods (i.e. scaled ID, DXA mass-driven ID, full DXA-driven ID, and DXA scaled ID) were compared using a repeated measures ANOVA with Tukey post-hoc tests. The major results were that 1) full DXA-driven participant specific inertial parameters differed from scaled inertial parameters 2) kinetic predictions significantly varied by method and 3) full DXA-driven ID predictions for shoulder compression force and shoulder internal rotation torque were significantly associated with BMI and/or SMI.

Keywords: Baseball, Biomechanics, DXA, Motion Analysis, Body Mass Index

ACKNOWLEDGMENTS

This work was supported by the W.M. Keck Foundation. Special thanks to Jordan Marthens and Dr. Scott Reaves for help processing and conducting DXA scans. Special thanks to Jay Sterner for helping recruit participants.

TABLE OF CONTENTS

Page

LIST OF TABLES

Table Page

LIST OF FIGURES

Figure Page

Chapter 1
INTRODUCTION

Youth baseball pitching arm injuries have steadily increased in recent years.[1] A number of studies have suggested that while governing bodies have implemented efforts such as pitch counts to combat this rise in injuries, the vast majority of young athletes participate in other leagues and/or travel teams.[2–4] Although athletes may be regulated in one league, the regulations are not enforced across leagues. Further, due to multiple teams schedules and season lengths, the lack of an off-season or lack of the four months of rest that is recommended by PitchSmart guidlines[5] puts young athletes at an increased injury risk from high and repetitive joint kinetics.

There is strong evidence that high and repetitive joint kinetics (i.e., forces and torques) are biomechanical mechanisms of pitching-related injuries.[1,6,7] These overuse injuries may begin during youth baseball; hence, improving the accuracy of pitching arm kinetic predictions may advance the development of injury prevention strategies. Pitching arm kinetics are commonly calculated using inverse dynamic (ID) analyses of motion analysis experiments. The ID analysis input parameters consist of body segment (e.g., hand, forearm, upper arm) masses, centers of mass, and radii of gyration, estimated as described below, as well as measured body segment accelerations. For youth[8,2] and adult pitching analyses[9], scaled ID analyses estimate body segment inertial parameters using measured body mass and arm lengths and scaling parameters based on adult cadaver studies.[10] However, adult and youth scaled mass ratios, center of mass ratios, and radii of gyration ratios have been shown to differ, especially for the upper arm segment.[11] Therefore, use of adult scaled inertial parameters may introduce considerable errors in ID predictions of youth pitching arm kinetics, especially in a participant-specific manner.

Parameter and/or ID analyses using dual energy X-ray absorptiometry (DXA) to measure participant-specific inertial parameters has been conducted in previous studies. In a study with Canadian Paralympic athletes, inertial parameters were calculated and found to be different than scaled values.[12] In a pitching study with 10-16 year-olds, multivariable regression analysis with kinetic parameters and participant specific masses from DXA predicted a direct relationship between body composition characteristics and injury related joint kinetics.[2] Additionally, in our

recent baseball pitching study with 10-11 year-olds, ID analyses with participant specific mass ratios and scaled inertial parameters predicted significant differences in shoulder compression force and shoulder internal rotation torque, with higher predictions from DXA mass ratios.[13] The corresponding explanation for both latter findings is that during the pitching motion the arm segments experience relatively high accelerations and, thus, body segment masses and composition have a greater effect on ID predictions of pitching arm kinetics. However, the first study [2] was limited because DXA data was only used in multiple variable regression analysis against kinetics and was not used in calculating the kinetics themselves. The second study [13] was limited because only the mass ratios of the arm segments, and not the inertial parameters, were calculated from DXA data. Thus, the first objective to this study was to calculate all 3D arm segment inertial parameters from DXA data and to use those parameters in ID analyses.

According to Pitch Smart guidelines[5], overweight measures (e.g. body weight, body mass index [BMI], etc.) have not been identified as risk factors for youth pitching injuries. However, there is evidence that being overweight and/or being obese increases injury risk for youth baseball players[14] and other youth sports participants.[15,16] In a recent study with 10- to 11-year old pitchers, use of DXA-mass driven ID, where pitching arm segment masses were determined from DXA scans, found that shoulder compressive force was correlated with BMI and both shoulder compressive force and elbow varus torque were correlated with total body mass.[13] Additionally, in several studies with 9- to 16-year-old pitchers, shoulder and elbow torques were shown to correlate with total body mass, BMI, and/or total fat and lean arm masses.[2,6,8] In comparison with other overweight measures, an advantage to considering BMI is that it is relatively easy to calculate and, thus, highly accessible to players, parents, and coaches. Thus, BMI is and has been used for associations with pitching arm kinetics. Thus, in this study, the second objective was to investigate associations between pitching arm kinetics and BMI.

Although previous studies have demonstrated associations between kinetic predictions and BMI, BMI may not be the most accurate measure to use because it is the masses (including both lean and fat masses) of only the pitching arm segments that ID uses to calculate pitching

arm kinetics. Thus, the third objective of this study was to investigate associations between pitching arm kinetics and a novel overweight measure termed segment mass index (SMI).

The hypotheses of this study were that, for 10- to 11-year-old baseball pitchers, (1) full DXA-driven ID and scaled ID inertial parameters would differ; (2) injury-related shoulder and elbow joint kinetics (shoulder compressive force, internal rotation torque, horizontal adduction torque; elbow varus torque) predicted by scaled (where parameters called from [10] are used for ID predictions), DXA mass-driven, and DXA scaled (where full-DXA inertial parameters are averaged across all participants and utilized for ID predictions) would, on average, differ; and (3) shoulder and elbow joint kinetics predicted by full DXA-driven ID would be significantly associated with BMI and SMI. Accordingly, this study was novel by developing an algorithm for calculating full 3D inertial parameters and by investigating associations with the novel overweight measure, SMI.

Chapter 2

METHODS

2.1 Participant Recruitment

Eighteen male participants (age 10.6 ± 0.5 years, height 147.8 ± 7.4 cm, body mass 39.6 ± 7.3 kg, BMI 18.0 ± 2.2 kg/m^2) with pitching experience during the preceding little league season and no recent history of pitching-related injuries participated. With the intent to represent the target population (i.e., 10- to 11-year-old youths with pitching experience in the preceding season) and meet randomness requirements for investigation of significant associations, no attempt was made to recruit pitchers of a specific BMI.

2.2 Informed Consent and DXA Scans

All DXA scans and experiments were conducted in conjunction with a previously published study.[13] Participants completed pre-game tests to measure body weight, height, and arm segment lengths, using a tape measure and standard scale. Then, participants underwent a DXA scan using a Lunar iDXA scanner (GE Healthcare, Madison, WI, USA). After the scan was completed, participants were offered healthy snacks, completed warm-up exercises, changed into compression clothing, and 38 retroreflective markers were placed on anatomical landmarks (see Appendix A) based on the PitchTrak software. Informed assent and consent were obtained from each participant and their legal guardian, respectively.

2.3 Experiments

Pitching experiments were completed and captured using a motion analysis system (Fig. 2.1). Marker trajectories were recorded in Cortex analysis software (Version 7.4.6, Motion Analysis, Santa Rosa, CA, USA) at 200 Hz, interpolated (third-order spline), and filtered (4th order Butterworth filter, cutoff frequency 12 Hz).[17] 10 pitches were recorded and the last 3 pitches with usable data for each participant were analyzed independently to obtain averaged values.

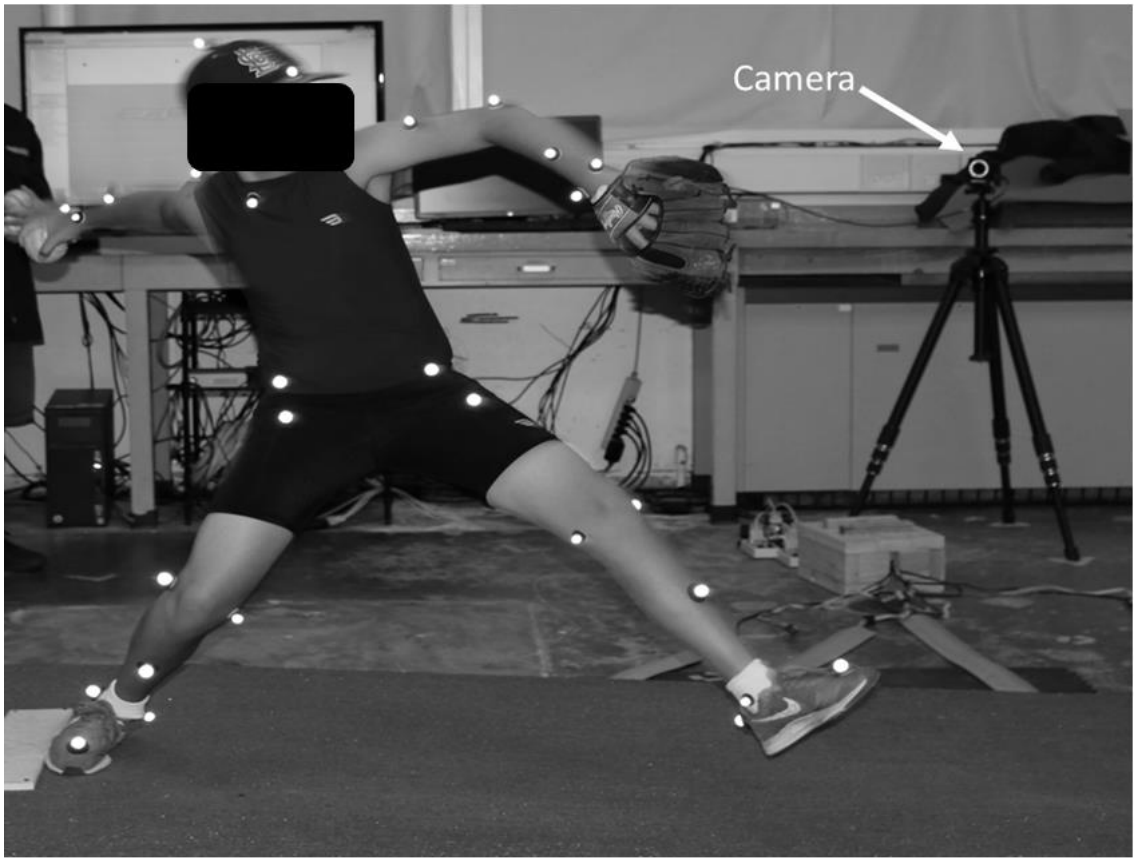

Figure 2.1: Participant pitching off portable pitching mound with retroreflective markers to capture kinematic data and 1 of 12 motion analysis cameras shown.

2.4 Analysis

After collecting raw data for the experiments in Cortex, all kinetics were calculated in PitchTrak (a subset of Cortex) with the specific inertial parameters dependent on the specific analysis.

2.4.1 Scaled Parameters

PitchTrak software uses scaled mass ratios, centers of mass, and radii of gyration as default values that are based on values found in cadaver studies[10], as was widely done in previous pitching studies.[18,19]

2.4.2 DXA Mass-Driven Parameters

DXA software (GE Healthcare) emits x-ray energy at two filtered levels that attenuate differently based upon tissue composition (bone mineral content, adipose, lean) on an

individualized pixel structure. The software adds pixel composition measures over a segmented region (e.g. arm, trunk) and reports total segment composition parameters. Also, the software produces 2 images: 1 with bone mineral density information and one with grouped (adipose and lean) soft tissue information.

As in a previous study[1], images were manually segmented into custom regions of interest for the pitching arm that agrees with a previous study that reported youth anthropometric data[11]: upper arm, forearm, and hand. (Fig. 2.2). The upper arm segment was defined from the shoulder joint center at the humeral head with its surrounding tissue to the elbow joint center at the humeral epicondyle. The forearm segment was defined from the humeral epicondyle to the styloid process and the hand segment was defined from the styloid process to the 3rd metacarpal. The DXA outputted mass ratios were then utilized as the DXA-mass driven mass ratios. The centers of mass and radii of gyration were kept constant between scaled and DXA mass-driven parameters. The DXA masses were formatted for use in PitchTrak with PitchTrak segment definitions[10] as follows: segment masses were converted to mass ratios by dividing by the total body mass; the mass of the ball (147 grams) was accounted for in the hand mass ratio, centers of mass were calculated as defined from the proximal joint center for use in PitchTrak, radii of gyration were converted to ratios by dividing by the segment length.

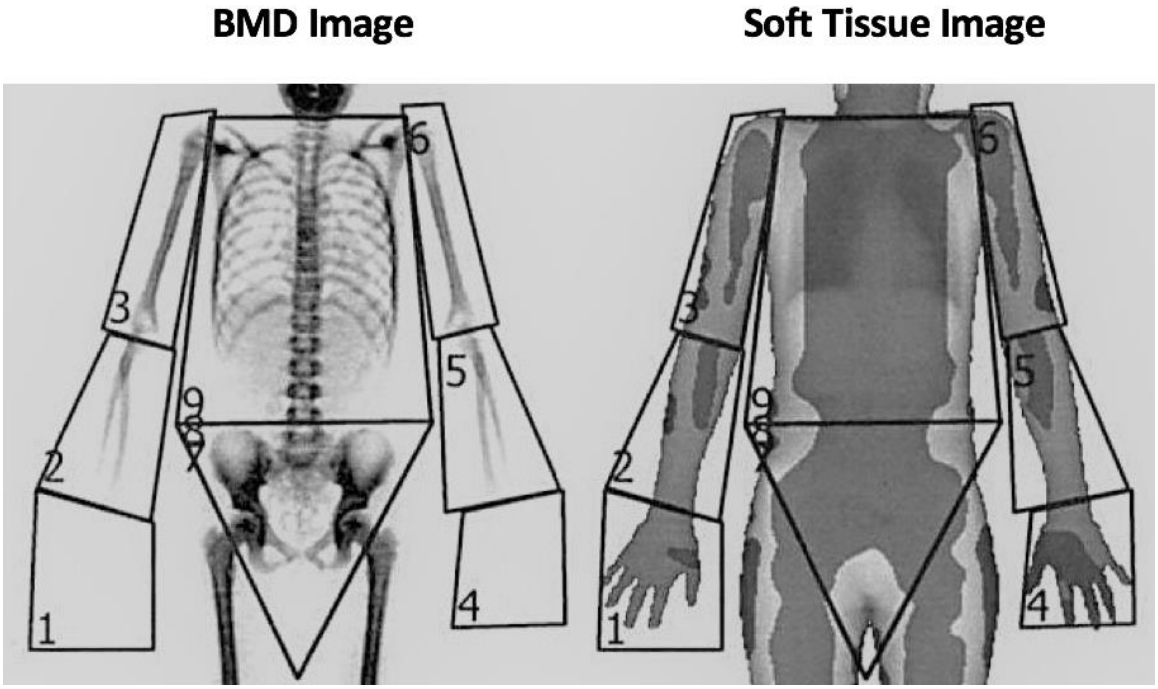

Figure 2.2: (Left) bone mineral density (BMD) and (right) soft tissue image of a youth participant. BMD scan: higher grayscale intensity indicates higher bone density. Soft tissue scan: higher grayscale intensity indicated lower body fat percentage. Regions 1 and 4 represent hands, regions 2 and 5 represent forearms, and regions 3 and 6 represent upper arms.

2.4.3 Full DXA-Driven Parameters

The DXA software's pixel information for each participant was exported for further analysis in MATLAB (MathWorks, Natick, MA, USA). Individual scan composition files contained an array of pixels (0.24 by 0.32 mm) for both the bone mineral density and soft tissue content.

For this study, a custom MATLAB code was written to calculate mass, center of mass, and radii of gyration for each arm segment. The customized code is outlined in the following steps for the upper arm (Fig. 2.3). The coordinate system was defined as follows: x is the mediolateral axis, y is the longitudinal axis, and z is the anteroposterior axis 1) Each pixel P_i was modeled as a point mass and its mass m_{P_i} was calculated using raw DXA values and packing factors.[20] The packing factors describe the needed conversion to give an individualized 2-dimensional pixel density ρ_{p_i} for each pixel in the array. Using the pixel width and height ($P_w,\ P_h$), the pixel mass was calculated using $m_{pi} = \rho_{pi} * (P_w * P_h)$. 2) The segment mass M was calculated by summing

all the pixel masses located in the segment: $M = \sum m_{pi}$. 3) The coordinates $(x_{p_{i/o}}, y_{p_{i/o}})$ of each pixel P_i relative to the pixel array origin O (which defaults to the upper left of the array at the first non-zero value) were used to calculate the coordinates (x_G, y_G) of the center of mass (G) relative to O using $x_G = \sum(m_{Pi} * x_{P_{i/o}})\ /M$ and $y_G = \sum(m_{Pi} * y_{p_{i/o}})\ /M$. The center of mass was assumed to lie in the X-Y plane so $z_G = 0$. These center of mass coordinates defined the origin G of a segment coordinate system with XYZ axes (Fig. 2.3). 4) The moment of inertia with respect to G about the anteroposterior Z axis (I_z) was calculated using $I_Z = \sum(m_{Pi} * d^2_{Pi/G})$, where $d_{p_{i/G}}$ is the distance of each pixel from G. 5) The anteroposterior axis radius of gyration (k_z) was calculated using $k_Z = (I_Z/M)^{1/2}$. The mediolateral axis radius of gyration (k_x) was assumed from symmetry about the Y-axis to be $k_x = k_z$. 6) The longitudinal axis radius of gyration about the Y axis (k_y) was assumed using the ratios of k_y/k_z reported in [21] to be $k_y = 0.55 * k_z$ for the upper-arm, $k_y = 0.47 * k_z$ for the forearm, and $k_y = 0.63 * k_z$ for the hand. 7) The custom code output variables were formatted for use in PitchTrak with PitchTrak segment definitions[10] similar to those defined in Section 2.4.2: segment masses were converted to mass ratios by dividing by the total body mass; the mass of the ball (147 grams) was accounted for in the hand mass ratio, centers of mass were calculated as defined from the proximal joint center for use in PitchTrak, radii of gyration were converted to ratios by dividing by the segment length.

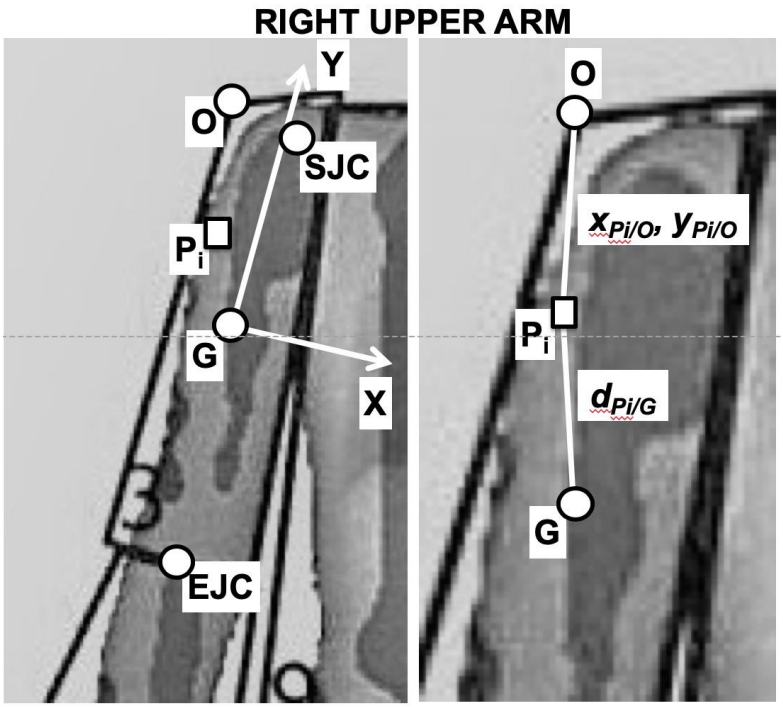

Figure 2.3: Inertial parameter calculation axes. (Left) Axes centered at mass center (G): longitudinal Y-axis through elbow (EJC) and shoulder (SJC) joint centers, medio-lateral X-axis directed through elbow epicondyles but located at G, anteroposterior Z-axis (not shown). O = pixel array origin, P_i = arbitrary pixel. (Right) Coordinates ($x_{p_{i/O}}, y_{p_{i/O}}$) of P_i relative to O and distance $d_{p_{i/G}}$ of P_i relative to G.

2.4.4 DXA Scaled Parameters

All 18 participants were evaluated using the code developed for full DXA-driven inertial parameters. Inertial parameters (mass ratios, centers of mass, and radii of gyration ratios) for each of the pitching arm segments were averaged. The averaged inertial parameters were then used as DXA scaled parameters for ID analysis of each participant.

2.4.5 Kinetics

All kinetic parameters were calculated in PitchTrak using scaled, full DXA-driven, DXA mass-driven, and DXA scaled parameters for each participant. Analyzed kinetic parameters included maximum values of shoulder compressive force, shoulder internal rotation torque, shoulder horizontal adduction torque, and elbow varus torque throughout the pitch cycle, which is

defined from foot contact to ball release (Fig. 2.4). Kinetic parameters were expressed as internal joint loads (e.g., an external elbow valgus torque produces an internal varus torque generated by tissues including the UCL[22]).

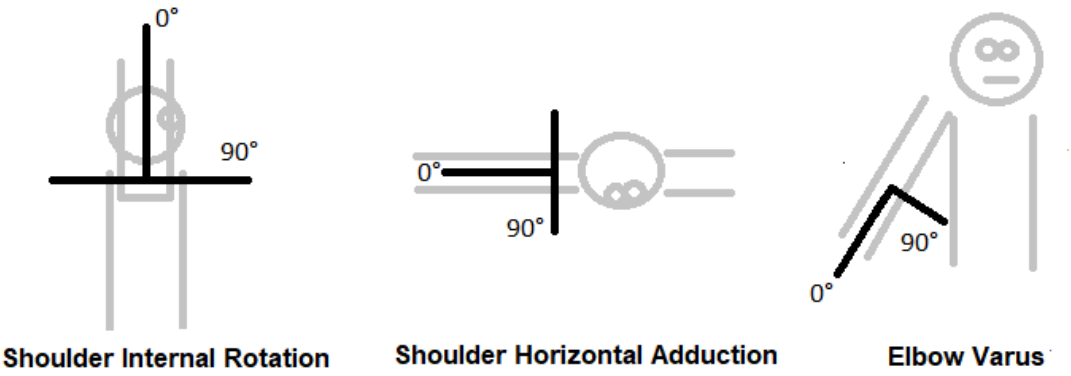

Figure 2.4: Schematic of PitchTrak angle definitions used for torque directions for a right-handed pitcher.

2.4.6 Statistical Analysis

One-sample t-tests were performed to determine significant differences between full DXA-driven inertial parameters and their respective scaled values. Since there were 6 parameters for each of the 3 segments of the arm, a Bonferroni correction factor of 18 was applied (significance defined as $p<0.0028$).

A repeated measures analysis of variance model with participant ID (1-18) as the random factor and measurement method (scaled ID, DXA mass-driven ID, full DXA-driven ID, and DXA scaled ID) as the fixed factor was fit to each kinetic parameter. Post hoc comparisons were performed to determine which measurement methods produced significantly different average measurements. Since there were 4 measurement methods, a Bonferroni correction of 4 was applied when analyzing these methods (significance defined as $p<0.0125$).

Six separate linear regression models were run to examine the association between each of the shoulder kinetic parameters predicted by full DXA-driven ID and BMI and Total Arm SMI. Total arm SMI is a participant measurement characterized by the total arm mass divided by the

total arm length. Several other formulae were considered; see the Discussion for more details. Two separate linear regression models were run to examine the association between the elbow kinetic parameter predicted by full DXA-driven ID and BMI and Lower Arm SMI (significance defined as $p<0.006$). Lower Arm SMI was defined similarly to Total Arm SMI, but with the lower arm mass and lower arm length.

Chapter 3

RESULTS

DXA and scaled inertial parameters differed for each of the arm segments (Table 4.1). For the upper arm, DXA mass ($p<0.001$), longitudinal and sagittal centers of mass ($p<0.001$), and transverse, longitudinal, and sagittal radii of gyration ($p<0.001$) were larger than their respective scaled parameters. For the hand, DXA mass ($p<0.001$), longitudinal and sagittal centers of mass ($p<0.001$), and sagittal and longitudinal radii of gyration were smaller than their respective scaled parameters ($p<0.001$). For the forearm, DXA mass($p<0.001$) and sagittal centers of mass ($p<.001$) were larger than their respective scaled values.

Table 4.1. **Scaled and DXA upper arm, forearm, and hand parameter ratios**, mean ± SD.

Notes. Segment masses are relative to body mass. Center of mass locations and radii of gyration are relative to segment length. [b] Scaled from McConville et al.[21] [*]= significant difference compared against scaled value, $p<0.001$

	Mass (%)		Medio-lateral Center of Mass (%)	
	Scaled	**DXA**	**Scaled**	**DXA**
Upper Arm	2.71	3.34 ± 0.26*	0	7.65 ± 1.49*
Forearm	1.62	1.51 ± 0.11*	0	4.32 ± 1.97*
Hand	0.61	0.66 ± 0.05*	0	6.22 ± 4.14*
	Longitudinal Center of Mass (%)		**Medio-lateral Radius of Gyration (%)**	
Segment	**Scaled**	**DXA**	**Scaled**	**DXA**
Upper Arm	57.7	41.3 ± 2.10*	28.5	33.8 ± 1.23*
Forearm	45.7	46.0 ± 2.51	27.6	27.1 ± 1.39
Hand	79.0	70.6 ± 6.17*	62.8	53.9 ± 4.87*
	Longitudinal Radius of Gyration (%)		**Anteroposterior Radius of Gyration (%) [b]**	
Segment	**Scaled**	**DXA**	**Scaled**	**DXA**
Upper Arm	15.8	18.7 ± 0.68*	26.9	33.8 ± 1.23*
Forearm	12.1	12.6 ± 0.96	26.5	27.1 ± 1.39
Hand	40.1	33.8 ± 4.39*	51.3	53.9 ± 4.87

Shoulder kinetic parameters (Table 4.2) varied between full DXA-driven ID and for compressive force ($p<0.001$), internal rotation torque ($p<0.001$), and horizontal adduction torque ($p<0.001$). Elbow varus torque ($p=0.831$) did not differ between methods.

Table 4.2. Shoulder and elbow kinetics calculated using scaled, DXA mass-driven, full DXA-driven, and DXA scaled ID, mean ± SD. *Note. *=significant difference when compared to the scaled ID value, p<0.001. **=significant difference when compared to DXA mass-driven ID value, p<0.001. No differences were found between full DXA-driven ID and DXA scaled ID.*

Shoulder	**Scaled ID**	**DXA mass-driven ID**	**Full DXA-driven ID**	**DXA scaled ID**
Compressive Force (N)	245± 56	258± 63	279± 74*, **	276± 82*
Internal Rotation Torque (N-m)	14.4± 4.1	15.2± 4.6	18.9± 6.3*, **	18.2± 6.5*, **
Horizontal Adduction Torque (N-m)	27.8± 11	29.1± 12	40.9± 22*, **	40.8± 23*, **
Elbow				
Varus Torque (N-m)	11.6±2.4	11.8± 2.5	11.8± 2.8	11.7± 2.7

Shoulder internal rotation torque ($p=0.005$) was positively correlated with BMI (Table 4.3). Shoulder compressive force ($p=0.002$) and shoulder internal rotation torque ($p=0.004$) were positively correlated with total arm SMI. No associations were found between shoulder horizontal abduction torque or elbow varus torque and BMI or Lower Arm SMI**.**

Table 4.3. Single linear regression results of full DXA-driven ID shoulder and elbow kinetics vs. BMI and SMI, R^2 (p-value). Note. *=significant association; p<0.006 defined significance

	BMI	SMI
Shoulder		**Total Arm SMI**
Compressive Force (N)	0.39 (0.040)	0.46 (0.002) *
Internal Rotation Torque (N-m)	0.24 (0.005) *	0.41 (0.004) *
Horizontal Adduction Torque (N-m)	0.27 (0.028)	0.29 (0.020)
Elbow		**Lower Arm SMI**
Varus Torque (N-m)	0.05 (0.375)	0.10 (0.191)

Chapter 4

DISCUSSION

There were several novel features of this study. First, this study used DXA scan data to calculate full 3D participant-specific inertial parameters of the pitching arm segments. Second, these parameters were used with a full DXA-driven ID method to calculate pitching arm kinetics. Third, the results were used to analyze associations between injury-related shoulder and elbow kinetics and a novel overweight classification of the pitching arm, SMI.

The results supported the first hypothesis that the full DXA-driven inertial parameters were different than their respective scaled values. One explanation for that result is that the scaled values are based on adult cadaver studies and it has been previously reported that child and adult anthropometric parameters differ.[13] Upper-arm inertial values presented the largest differences, presumably due to the fact that the full DXA-driven segment definition, which agrees with some previous studies[11,13] but not others[10,21], included additional upper arm mass superior and inferior to a transverse plane through the shoulder joint center. The additional upper arm mass is likely to have shifted the medio-lateral center of mass off the longitudinal axis, as most of the shoulder mass added is not symmetric about the longitudinal axis. Furthermore, this additional mass directly affects the three radii of gyration about the center of mass by shifting the mass distribution about each axis. Forearm and hand inertial parameters presented smaller differences than the upper arm. This is likely due to the extra mass the upper arm definition includes when compared to standard definitions.

The differences in the three full DXA-driven radii of gyration and scaled radii of gyration for each pitching arm segment varied. The upper arm radii of gyration about each axis were higher than scaled values, while the full DXA-driven medio-lateral center of mass was larger, and the full DXA-driven longitudinal center of mass was smaller than their respective scaled values. The included shoulder soft tissue mass shifts the center of mass toward the proximal endpoint and is likely the cause of the lower longitudinal center of mass ratios. As for the medio-lateral center of mass, previous studies assumed this to lie on the longitudinal axis[10], however with DXA data this assumption was not valid and the medio-lateral center of mass was calculated to be

close to, but not on, the longitudinal axis. Next, the forearm radii of gyration and longitudinal center of mass did not present statistically different values as compared to the scaled values. Again, as was the same for the upper arm and hand, the medio-lateral center of mass was presumably different as it did not lie along the longitudinal axis. Lastly, the hand radii of gyration varied depending on the plane. Scaled radii of gyration along the medio-lateral and anteroposterior axes were assumed to be the same, which likely is erroneous when applied to the hand as opposed to the forearm and upper arm. Geometrically, the forearm and upper arm are close to axisymmetric when examining how the mass of the segment is distributed in each of the axes. In the hand, higher values were presented along the anteroposterior axis, but lower values were presented along the medio-lateral axis when compared to scaled values. This is most likely due to this symmetry assumption.

The results supported the second hypothesis as scaled, DXA mass-driven ID, full DXA-driven ID, and DXA scaled ID predicted different shoulder, but not elbow, kinetics. Shoulder kinetic parameters (compressive force, internal rotation torque, and horizontal adduction torque) were higher when using full DXA-driven and DXA scaled ID than scaled and DXA mass-driven ID, with the largest differences found for the upper arm. An explanation for this is that this study and previous studies[13,23,24] used the standard segment definitions for each of the arm-segments in the scaled ID analysis; however, this study used the additional upper arm mass for DXA mass-driven, full DXA-driven, and DXA scaled ID. The additional upper arm mass included tissues surrounding the shoulder that appear to rotate around the shoulder joint center during the pitching motion and appears to contribute to shoulder kinetic predictions and, therefore, should be included in the upper arm segment mass for more accurate predictions. This additional mass resulted in the largest inertial parameter differences being in the upper arm. The ID analysis that PitchTrak uses calculates joint loads and torques by going from the distal to the proximal joint centers, where the calculated kinetics at each joint center (elbow, and shoulder) are then dependent only on the inertial parameters for the segments distal to that joint. Thus, higher inertial parameters in the upper arm contribute to only the joint kinetics in the shoulder joint.

Furthermore, no differences were predicted between scaled and DXA mass-driven ID kinetic predictions as there were in a previous study($p<0.002$ [13] vs $p<0.025$ for this study). A likely explanation for this is that the repeated measure analysis of variance now contains more methods and inter-method variability. The increased variability shifts the significance threshold, which is likely now why we don't see significance between scaled and DXA mass-driven ID predictions.

The results supported the third hypothesis as shoulder and elbow kinetics were associated with BMI and SMI. The positive associations between shoulder compressive force and internal rotation torque with BMI and/or SMI appear to be reasonable, because independent analyses done in another study revealed that pitching arm masses were positively correlated with BMI.[13] As various studies have suggested kinetics may also depend on BMI[8,13]. In addition to these results, this study presents SMI associations that were much stronger than BMI associations (Appendix F). This is likely because SMI calculations only consider the relative arm segment masses, while BMI includes the total body mass.

This study provides several implications for youth baseball players. Common pitching injuries include ulnar collateral ligament (UCL) sprain, that has been linked to high elbow varus torque[25,26], and shoulder rotator cuff and labrum injuries, which have been linked to high horizontal abduction torque, internal rotation torque, and compression force.[23,27–29] Thus, a clinically relevant result is that the full DXA-driven ID methods predicted different inertial parameters and shoulder kinetics when compared to scaled ID. The use of participant-specific inertial parameters, which are tailored to youth anthropometry, likely leads to more accurate kinetic predictions of injury-related pitching arm kinetics and, thus, may lead to an improved understanding of injury risk factors. Moreover, when participant-specific accuracy is the focus of a pitching biomechanics study, full DXA-driven ID becomes more imperative as differences between scaled and full DXA-driven ID were as high as 76% for shoulder internal rotation torque and nearly 25% for elbow varus torque for some participants, and differences between scaled and DXA scaled ID were as high as 79% for shoulder internal rotation torque and nearly 9% for elbow varus torque. However, due to DXA scan availability being low, studies involving groups of

youth pitchers may consider utilizing DXA scaled parameters (i.e. the average inertial property ratios from Table 1), noting the large individual differences, as they were shown to significantly predict higher kinetics that resemble those predicted via full DXA-driven ID analyses. In addition, the current study reported significant increases (as much as 25% for individual participants) in predictions of joint kinetics with full DXA-driven ID, and it may even be that with older participants, differences are higher due to higher masses and heights.

A second clinically relevant result was that, for 10- to 11-year-old pitchers, shoulder internal rotation torque was significantly associated with BMI and both shoulder compressive force and shoulder internal rotation torque were significantly associated with SMI. During the past three decades, prevalence rates of childhood and adolescent obesity have more than doubled in the United States.[30] In particular, while overweight and obesity prevalence in youth baseball is similar to the general youth population[31–33], it is higher than most other youth sports[14,34,35] most likely due to the sport containing relatively low vigorous activity and caloric expenditure[31,36], in addition to an unhealthy food culture[37]. While BMI appears to be a reliable predictor of injury-related kinetics in youth pitchers[2,8], a recent study found that shoulder kinetics were much more strongly correlated with arm mass than total body mass.[13] Accordingly, SMI, which considers just the total arm mass, appeared to be an overweight measure that is an even better predictor of injury-related pitching arm kinetics than BMI. This is explained through the higher associations found between most pitching arm kinetics and SMI. Thus, pitchers with higher SMI, whether due to excessive fat or muscle mass, may be at more risk for shoulder injury. This observation agrees with an explanation of the inverse dynamic approach: shoulder kinetics only depend explicitly on upper arm, forearm, and hand inertial parameters, so a measure of whether the arm is overweight should produce stronger associations than with total body BMI.

There are several limitations in the current study. First, the pitching distance was limited to 25 feet due to the lab size. Second, the number of participants, especially overweight and obese participants, was limited because participants were selected at random and not selected based on body type. However, it should be noted that the percentage of overweight to obese pitchers corresponded well to the actual percentage of overweight to obese youth baseball

pitchers.[31,33] Third, DXA data provides 3-D mass data within a 2-D image of the coronal plane by condensing the density data along the anterior-posterior axis (shown in Fig. 2.3) to an average density for that specific pixel, P_i. Therefore, this study had to make assumptions about the 3-D mass distribution in the sagittal and transverse planes. However, it is likely that the inertial parameters from the DXA data were more accurate than the scaled values due to the use of participant specific DXA data and the fact that scaled values were based on other limiting assumptions.[10] Lastly, a limitation was uncertainty regarding the exponent of the length term used in the definition of SMI. SMI was defined in a manner analogous to BMI and, thus, quantified whether the pitching arm segment is "overweight." More specifically, SMI was defined by total segment mass divided by total segment length. For BMI (body mass divided by height squared), the exponent on height is two and was chosen so that BMI is an index for excessive adiposity of the total body. In contrast, here the SMI parameter is defined to be an overweight measure of the pitching arm, including both lean and fat mass, and is intended to be an index for pitching arm kinetics. For this study, we examined using exponents of both one and two, and found that an exponent of 1 was a much better predictor of both shoulder internal rotation and elbow varus torques (Appendix F). Therefore, this paper only reports results with an SMI exponent of one.

Although efforts are being made to improve injury prevention by limiting youth baseball pitchers, continued efforts are needed as the popularity of travel or tournament teams counteracts the implemented regulations in certain leagues. While full DXA-driven ID analysis adds to improvement of research prevention in that they are the only analysis known to use calculated 3D inertial parameters on a participant-specific basis, there still is a need to improve other variables used in Euler's Equations to make ID predictions. Input variables in Euler's equation for the sum of forces includes three segment masses, the 3-D location of the center of mass, and the three accelerations of the three segment centers of mass while the output variable is the joint force. Input variables in Euler's equation for the sum of moments includes the 3-D location of the center of mass, a moment arm from the center of mass to the joint center, the three radii of gyration, three segment masses, three segment angular velocities and three segment angular accelerations while the joint torques are output variables. In this study, advancements were made

in predicting more accurate kinetics by improving the three segment masses and the location of centers of mass on the medio-lateral and longitudinal planes in Euler's sum of forces equation and improving three segment masses, anteroposterior radii of gyration, and the location of the center of mass on the medio-lateral and longitudinal planes in Euler's sum of moments equation. However, there is still a need present to improve calculations of anteroposterior center of mass, medio-lateral and longitudinal radii of gyration due to assumptions of segment symmetry and scaling ratios. In addition, segment acceleration, angular velocity, and angular acceleration capture methods (i.e. capture rate, number of cameras, quality of data, etc.) could be improved due to troublesome marker visibility. Continued efforts to improve these calculations can help determine if the youth baseball pitchers are at higher injury risk based upon overuse and overweight measures.

In summary, the current study was the first to investigate youth pitching arm kinetics calculated with participant specific DXA upper arm, forearm, and hand inertial parameters. Novel results for 10 -11 year old pitchers were: (1) DXA upper arm, forearm, and hand inertial parameters were different than their respective scaled masses; (2) full DXA driven ID predicted higher shoulder kinetic parameters than scaled ID and DXA mass-driven ID;(3) there were no significant differences was present when comparing full DXA-driven ID to DXA scaled ID; (4) there existed associations between shoulder kinetics and BMI and/or SMI. These novel results suggest that full DXA-driven ID more accurately predicts shoulder forces and torques than scaled ID and DXA-mass ID for youth baseball pitchers. Therefore, if participant specific DXA inertial parameters cannot be calculated, the average inertial parameters reported here should be considered when performing ID calculations with this age group. Further, our study presents a new body composition measure, SMI, that appears to be an overweight measure that serves as a better index of injury-related pitching arm kinetics than total body BMI.

REFERENCES

[1] Fleisig GS, Andrews JR. Prevention of elbow injuries in youth baseball pitchers. *Sports Health*. 2012;4(5):419-424.

[2] Garner JC, Macdonald C, Wade C, Johnson A, Ford MA. The influence of body composition on youth throwing kinetics. *Pediatr Exerc Sci*. 2011;23:379-387.

[3] Yang J, Mann BJ, Guettler JH, et al. Risk-Prone Pitching Activities and Injuries in Youth Baseball. *Am J Sports Med*. 2014;42(6):1456-1463. doi:10.1177/0363546514524699.

[4] Bohne C, George SZ, Jr GZ. KNOWLEDGE OF INJURY PREVENTION AND PREVALENCE OF RISK FACTORS FOR THROWING INJURIES IN A SAMPLE OF YOUTH BASEBALL PLAYERS. *Int J Sports Phys Ther*. 2015;10(4):464-475.

[5] Pitch Smart. http://m.mlb.com/pitchsmart/risk-%0Afactors/. Accessed November 18, 2019.

[6] Sabick MB, Torry MR, Lawton RL, Hawkins RJ. Valgus torque in youth baseball pitchers: A biomechanical study. *J Shoulder Elb Surg*. 2004;13(3):349-355. doi:10.1016/j.jse.2004.01.013.

[7] Anz AW, Bushnell BD, Griffin LP, Noonan TJ, Torry MR, Hawkins RJ. Correlation of torque and elbow injury in professional baseball pitchers. *Am J Sports Med*. 2010;38(7):1368-1374. doi:10.1177/0363546510363402.

[8] Darke JD, Dandekar EM, Aguinaldo AL, Hazelwood SJ, Klisch SM. Effects of Game Pitch Count and Body Mass Index on Pitching Biomechanics in 9- to 10-Year-Old Baseball Athletes. *Orthop J Sport Med*. 2018;6(4):1-10. doi:10.1177/2325967118765655.

[9] Fleisig GS, Barrentine SW, Zheng N, Escamilla RF, Andrews JR. Kinematic and kinetic comparison of baseball pitching among various levels of development. *J Biomech*. 1999;32(12):1371-1375. doi:10.1016/S0021-9290(99)00127-X.

[10] De Leva P. Adjsutments to Zatsiorsky-Seluyanov's Segment Inertia Parameters. *J Biomech*. 1996;29(9):1223-1230.

[11] Jensen RK. Body segment mass, radius and radius of gyration proportions of children. *J Biomech*. 1986;19(5):359-368. doi:10.1016/0021-9290(86)90012-6.

[12] Ganley KJ, Powers CM. Anthropometric parameters in children: A comparison of values obtained from dual energy x-ray absorptiometry and cadaver-based estimates. *Gait Posture*. 2004;19(2):133-140. doi:10.1016/S0966-6362(03)00038-9.

[13] Sterner J, Reaves S, Aguinaldo A, Hazelwood S, Klisch S. DXA-driven inverse dynamics of pitching arm kinetics in youth baseball pitchers. *Sport Biomech*. 2020;In Press. doi:doi.org/10.1080/14763141.2020.1715470.

[14] Yard E, Comstock D. Injury Patterns by Body Mass Index in US High School Athletes. *J Phys Act Heal*. 2016. doi:10.1123/jpah.8.2.182.

[15] Gómez JE, Ross SK, Calmbach WL, Kimmel RB, Schmidt DR, Dhanda R. Body fatness and increased injury rates in high school football linemen. *Clin J Sport Med*. 1998;8(2):115-120. doi:10.1097/00042752-199804000-00010.

[16] Tyler TF, Mchugh MP, Mirabella MR, Mullaney MJ, Nicholas SJ. Risk Factors for Noncontact Ankle Sprains in High School Football Players. *Am J Sports Med*. 2006;34(3):471-475. doi:10.1177/0363546505280429.

[17] Matsuo T, Matsumoto T, Takada Y, Mochizuki Y. Influence of different shoulder Abduction

Angels during Baseball Pitching on Throwing Performance and Joint Kinetics. *17th Int Symp Biomech Sport*. 1999:389-392.

[18] Aguinaldo AL, Buttermore J, Chambers H. Effects of upper trunk rotation on shoulder joint torque among baseball pitchers of various levels. *J Appl Biomech*. 2007;23(1):42-51.

[19] Darke J, Dandekar EM, Aguinaldo AL, Hazelwood SJ, Klisch SM. Elbow and shoulder joint torques are correlated with body mass index but not game pitch count in youth baseball pitchers. In: *Summer Biomechanics, Bioengineering & Biotransport Conference*. ; 2017.

[20] GE Healthcare. Lunar -enCORE-based X-ray Bone Densitometer User Manual. 2010;(I).

[21] Mcconville JT, Churchill T. Anthropometric Relationships of Body and I. *Report*. 1980;105(21):7405-7409. doi:10.1073/pnas.0710346105.

[22] Buffi JH, Werner K, Kepple T, Murray WM. Computing muscle, ligament, and osseous contributions to the elbow varus moment during baseball pitching. *Ann Biomed Eng*. 2015;43(2):404-415. doi:10.1007/s10439-014-1144-z.

[23] Fleisig GS, Andrews JR, Dillman CJ, Escamilla RF. Kinetics of Baseball Pitching with Implications About Injury Mechanisms. *Am J Sports Med*. 1995;23(2):233-239. doi:10.1177/036354659502300218.

[24] Fleisig GS, Diffendaffer AZ, Ivey B, et al. Changes in Youth Baseball Pitching Biomechanics: A 7-Year Longitudinal Study. *Am J Sports Med*. 2018;46(1):44-51. doi:10.1177/0363546517732034.

[25] Andrews JR, Heggland EJH, Fleisig GS, Zheng N. Relationship of ulnar collateral ligament strain to amount of medial olecranon osteotomy. *Am J Sports Med*. 2001;29(6):716-721.

[26] Erickson BJ, Nwachukwu BU, Rosas S, et al. Trends in medial ulnar collateral ligament reconstruction in the United States: A retrospective review of a large private-payer database from 2007 to 2011. *Am J Sports Med*. 2015;43(7):1770-1774. doi:10.1177/0363546515580304.

[27] Fleisig GS, Andrews JR, Cutter GR, et al. Risk of serious injury for young baseball pitchers: a 10-year prospective study. *Am J Sports Med*. 2011;39(2):253-257. doi:10.1177/0363546510384224.

[28] Fleisig GS, Barrentine SW, Escamilla RF, Andrews JR. Biomechanics of overhand throwing with implications for injuries. *Sport Med*. 1996;21(6):421-437. doi:10.2165/00007256-199621060-0004.

[29] Barrentine SW, Fleisig GS, Whiteside JA, Escamilla RF, Andrews JR. Biomechanics of Windmill Softball Pitching With Implications About Injury Mechanisms at the Shoulder and Elbow. *J Orthop Sport Phys Ther*. 2013. doi:10.2519/jospt.1998.28.6.405.

[30] Cali AMG, Caprio S. Obesity in Children and Adolescents. *J Clin Epidemiol*. 2008;93(November):31-36. doi:10.1210/jc.2008-1363.

[31] Elkins WL, Cohen DA, Koralewicz LM, Taylor SN. After school activities, overweight, and obesity among inner city youth. *J Adolesc*. 2004. doi:10.1016/j.adolescence.2003.10.010.

[32] Nelson TF, Stovitz SD, Thomas M, LaVoi NM, Bauer KW, Neumark-Sztainer D. Do youth sports prevent pediatric obesity? A systematic review and commentary. *Curr Sports Med Rep*. 2011. doi:10.1249/JSR.0b013e318237bf74.

[33] Choate N, Forster C, Almquist J, Olsen C, Poth M. The Prevalence of Overweight in Participants in High School Extramural Sports. *J Adolesc Heal*. 2007. doi:10.1016/j.jadohealth.2006.09.014.

[34] Leek D, Carlson JA, Cain KL, et al. Physical activity during youth sports practices. *Arch Pediatr Adolesc Med*. 2011. doi:10.1001/archpediatrics.2010.252.

[35] Turner RW, Perrin EM, Coyne-Beasley T, Peterson CJ, Skinner AC. Reported Sports Participation, Race, Sex, Ethnicity, and Obesity in US Adolescents From NHANES Physical Activity (PAQ_D). *Glob Pediatr Heal*. 2015. doi:10.1177/2333794x15577944.

[36] Jetté M, Sidney K, Blümchen G. Metabolic equivalents (METS) in exercise testing, exercise prescription, and evaluation of functional capacity. *Clin Cardiol*. 1990.

[37] Irby MB, Drury-Brown M, Skelton JA. The Food Environment of Youth Baseball. *Child Obes*. 2016. doi:10.1089/chi.2013.0161.

[38] Laschowski B, McPhee J. Body segment parameters of Paralympic athletes from dual-energy X-ray absorptiometry. *Sport Eng*. 2016;19(3):155-162. doi:10.1007/s12283-016-0200-3.

APPENDIX A: PitchTrak Marker Set

The complete PitchTrak marker (Figure A.1) set utilized for all participants is based upon their dominant (or throwing) arm. The only different marker for right vs left-handed pitchers was the hand marker on the pitching arm. 38 total markers were used on every participant.

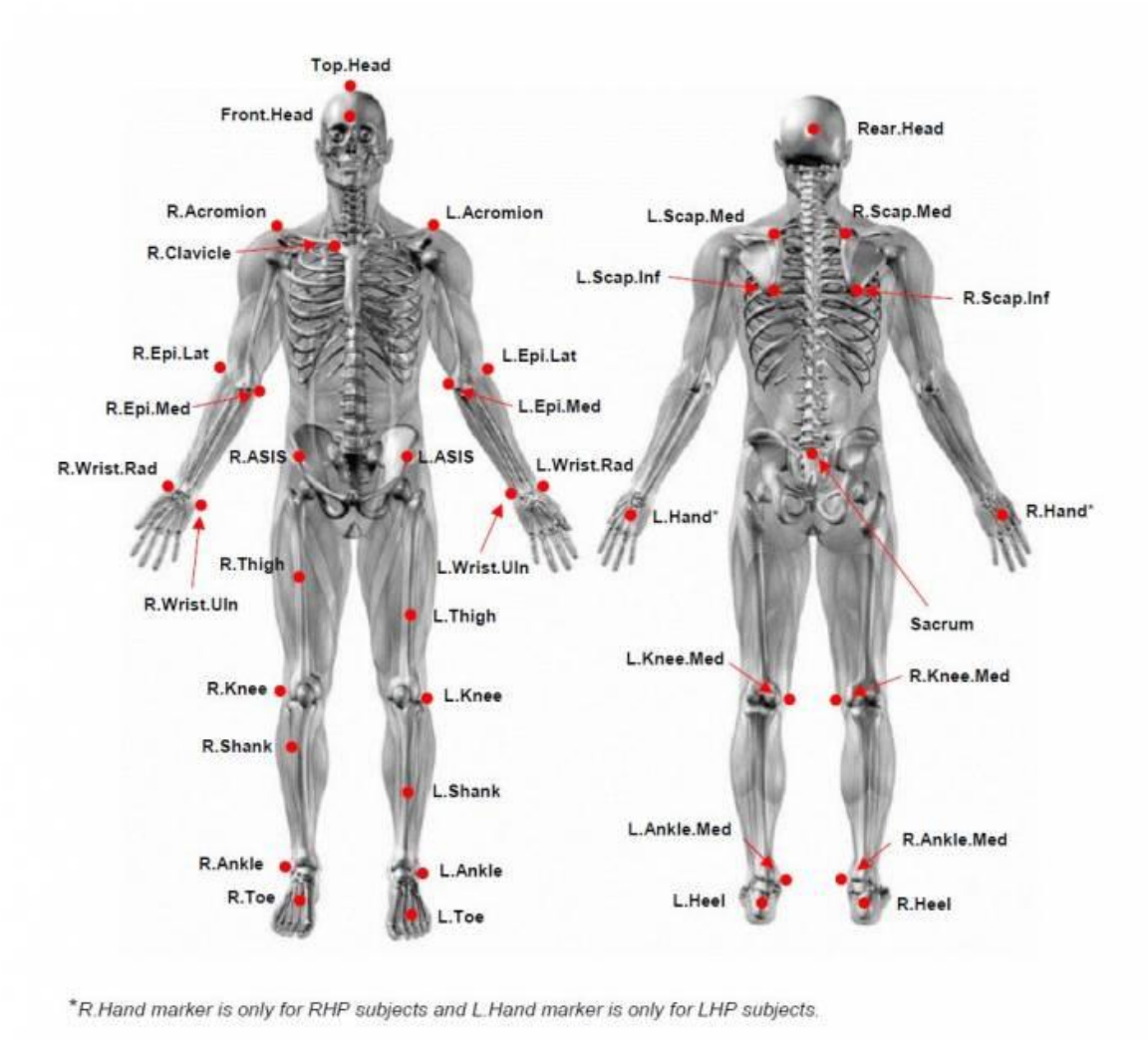

Figure A.1 – PitchTrak marker set for a right-handed pitcher.

Right Handed Pitcher: The marker set consisted of: top head, front head, back head, left acromium, right acromium, right clavicle, right medial scapula, right inferior scapula, left medial scapula, right inferior scapula, left lateral epicondyle, left medial epicondyle, left radial wrist, left ulnar wrist, right lateral epicondyle, right medial epicondyle, right radial wrist, right ulnar wrist, right hand, right asis, sacral, left asis, right thigh, right knee, right shank, right ankle, right heel,

right toe, left thigh, left knee, left shank, left ankle, left heel, left toe, right knee medial, right ankle medial, left knee medial, and left ankle medial.

Left Handed Pitcher: The marker set consisted of: top head, front head, back head, left acromium, right acromium, left clavicle, right medial scapula, right inferior scapula, left medial scapula, right inferior scapula, left lateral epicondyle, left medial epicondyle, left radial wrist, left ulnar wrist, right lateral epicondyle, right medial epicondyle, right radial wrist, right ulnar wrist, left hand, right asis, sacral, left asis, right thigh, right knee, right shank, right ankle, right heel, right toe, left thigh, left knee, left shank, left ankle, left heel, left toe, right knee medial, right ankle medial, left knee medial, and left ankle medial.

APPENDIX B: Code Validation

The following explanation of code validation was obtained from Colin Brown, part of a research group at the University of Waterloo. This research group has developed and utilized a similar pixelated MATLAB approach to post-processing raw iDXA data to get moments of inertia for a study published on the body segment inertial parameters of Paralympic athletes. [38] To validate the code, they obtained results and compared them with the results from the code outlined in Chapter 2.4.3. A full description obtained from Colin Brown of Waterloo follows:

A custom program was developed [Waterloo] to calculate body segment inertial parameters from the raw data measured by an iDXA full-body scan. The purpose of this endeavor was to obtain an accurate calculation of the moment of inertia of a body segment from iDXA data, as the iDXA proprietary software only outputs the mass of a body segment. An iDXA body scan outputs a variety of data to help identify different tissue types. For each type of body scan, the data is output in a two-dimensional array of 16-bit integers. Each pixel of the data represents a small segment of the body with a known physical area provided by the DXA scan pixel size. The numerical value of each data element is converted to a mass-areal density through the multiplication of a manufacturer-provided calibration factor. To determine the total mass parameters of a given segment of the body, the two scan types used were the Bone Mineral Density scan, and the Tissue scan (includes lean and fat body composition).

From the full-body scan data, the data obtained by [38] of the upper right arm was selected as a case study to compare with the calculated mass results by the iDXA software of the same study. Since the upper right arm was segmented manually from the full body scan by Laschowski, the same method described by Laschowski was applied to obtain the upper right arm data for this case study using the Tissue iDXA image as the reference. The segment coordinates were then used to crop the Bone Mineral Density scan from the full body scan data set. The segmented Bone Mineral Density and Tissue data files were prepared for the algorithm by multiplying with the respective calibration factor to obtain the mass density of each pixel. The mass of each of pixel was then obtained by multiplying with the known pixel dimension. The total

mass of the upper right arm segment was then obtained by summing the total mass of each pixel for both the Bone Mineral Density and Tissue data files. The close comparison between the mass calculated by the iDXA from [38] and the mass determined from the custom code of this case study is shown in the table below (Two scans for each subject were obtained by [38], and the average and standard deviation values are compared).

Using the first moment of mass formula (Equation B-1),

$$COM = \frac{\sum_{n=1}^{N} l_n m_n}{M} \quad \text{(B-1)}$$

the knowledge of the known pixel dimensions to define the relative distance from a predefined origin along with the mass of each pixel was used to calculate the center of mass of the segment. Using the assumption of a cylinder shape for the upper right arm, the parallel axis theorem, in combination with the previously calculated COM, was then applied to calculate the moment of inertia of the limb segment. These results are compared to the cadaver scaled results presented by [38] from the same iDXA data set (Fig B.1). The subjects were designated by ID's A1-A6.

From the validation of the approach described above due to the close comparison of calculated masses with the iDXA software and widely used cadaver scaled masses determined by [38], this approach was selected to verify the results of the custom code developed in this [Dalton's] study. The iDXA data obtained by [Dalton] was captured using the same iDXA scanner as the one used by [Waterloo]. To validate the results obtained by [Dalton], the upper arm segment coordinates determined by [Dalton] were used to segment the data for the input to the [Waterloo] custom code. To maintain consistency, the same x-y coordinate system used by [Dalton] was used in the [Waterloo] program, as well as the same calibration factor and pixel size. With the consistent parameters used and same upper limb segment input to the [Waterloo] program, the mass and MOI results matched those produced by [Dalton's] code*. (Fig B.1)

Mass (kg)	A1	A2	A3	A4	A5	A6
[1]	3.521 ± 0.173	2.533 ± 0.017	3.799 ± 0.381	3.319 ± 0.012	3.099 ± 0.192	2.431 ± 0.035
Matlab	3.540 ± 0.011	2.536 ± 0.001	3.811 ± 0.034	3.352 ± 0.049	3.071*	2.374 ± 0.022

MOI (kgm²)	A1	A2	A3	A4	A5	A6
[1]	0.026 ± 0.001	0.015 ± 0.001	0.034± 0.008	0.024± 0.001	0.024 ± 0.002	0.020 ± 0.001
Matlab	0.018 ± 2e-4	0.012 ± 4e-4	0.0223 ± 4e-4	0.017 ± 0.002	0.016*	0.0125 ± 5e-4

* Only one scan available

1. (Laschowski, B.; McPhee, J. Body segment parameters of Paralympic athletes from dual-energy X-ray absorptiometry. *Sports Eng.* **2016**, 19, 155-162)

Figure B.1 – Mass and Moment of Inertia Comparison between Waterloo code results ([1]) and this study's code results (Matlab).

APPENDIX C: Participant Specific Inertial Parameters

Table C.1 – Complete participant specific inertial parameters obtained from full DXA-driven code. Coordinate system defined as follows: x is the medio-lateral axis, y is the longitudinal axis, and z is the anteroposterior axis. Mean and Standard Deviation (SD) provided matches Table 4.1.

Participant	Percent Mass*	COM(X)	COM(Y)	COM(Z)	ROG(X)	ROG(Y)	ROG(Z)
2017Jul19-01	0.035	0.062	0.424	0.000	0.335	0.186	0.335
2017Jul19-02	0.033	0.080	0.426	0.000	0.343	0.190	0.343
2017Jul21-01	0.031	0.057	0.431	0.000	0.352	0.195	0.352
2017Jul21-02	0.029	0.081	0.419	0.000	0.337	0.187	0.337
2017Jul26-01	0.033	0.085	0.407	0.000	0.341	0.189	0.341
2017Jul27-01	0.037	0.077	0.419	0.000	0.359	0.199	0.359
2017Jul27-02	0.034	0.062	0.421	0.000	0.346	0.192	0.346
2017Aug20-01	0.033	0.067	0.448	0.000	0.325	0.180	0.325
2017Aug20-02	0.030	0.057	0.445	0.000	0.332	0.184	0.332
2017Aug20-03	0.039	0.095	0.386	0.000	0.336	0.186	0.336
2017Sep07-02	0.033	0.074	0.413	0.000	0.356	0.197	0.356
2017Sep30-01	0.036	0.097	0.411	0.000	0.336	0.186	0.336
2018Aug01-02	0.035	0.090	0.401	0.000	0.337	0.187	0.337
2018Aug13-01	0.034	0.111	0.431	0.000	0.302	0.167	0.302
2018Aug15-01	0.031	0.078	0.408	0.000	0.320	0.178	0.320
2018Aug16-01	0.034	0.068	0.380	0.000	0.312	0.173	0.312
2018Nov07-01	0.035	0.068	0.380	0.000	0.311	0.172	0.311
2018Nov09-01	0.034	0.068	0.380	0.000	0.319	0.177	0.319
Mean	0.034	0.077	0.413	0.000	0.333	0.185	0.333
SD	0.002	0.015	0.020	0.000	0.015	0.009	0.015

APPENDIX D: Inertial Parameter Effect on Inverse Dynamic Kinetic Predictions

Inertial Parameter effect on kinetic predictions was analyzed using the upper arm segment. Inertial parameters ($Segment\ Mass$, COM_x, COM_y, ROG_x, ROG_y, ROG_z) for the forearm and hand were held constant while the upper arm inertial parameters were changed one at a time, while keeping the others at the scaled values. Results (Tables D.1-4) for four pitching injury-related kinetic parameters (SIRT, SHAT, SCF, and EVT) are reported for each of the inertial values changed.

Table D.1 – Shoulder Internal Rotation Torque normalized (by body weight*height) results with mean and standard deviation (SD) for each specific inertial parameter changed. Coordinate system defined as follows: x is the medio-lateral axis, y is the longitudinal axis, and z is the anteroposterior axis.

	Inertial Parameter Changed							
Participant	***Segment Mass***	COM_x	COM_y	ROG_x	ROG_y	ROG_z	***All***	***None***
2017Jul19-01	0.021	0.022	0.021	0.022	0.022	0.021	0.024	0.018
2017Jul19-02	0.022	0.022	0.022	0.023	0.023	0.021	0.022	0.022
2017Jul21-01	0.019	0.020	0.019	0.020	0.029	0.018	0.030	0.018
2017Jul21-02	0.020	0.020	0.020	0.021	0.021	0.021	0.025	0.020
2017Jul26-01	0.024	0.029	0.029	0.030	0.029	0.028	0.034	0.023
2017Jul27-01	0.019	0.020	0.019	0.020	0.020	0.019	0.026	0.018
2017Jul27-02	0.024	0.023	0.022	0.022	0.027	0.021	0.036	0.023
2017Aug20-01	0.018	0.018	0.018	0.018	0.018	0.018	0.021	0.018
2017Aug20-02	0.018	0.018	0.018	0.019	0.018	0.018	0.019	0.018
2017Aug20-03	0.026	0.026	0.026	0.026	0.026	0.025	0.027	0.024
2017Sep07-02	0.026	0.028	0.027	0.028	0.027	0.026	0.034	0.025
2017Sep30-01	0.021	0.023	0.019	0.019	0.026	0.019	0.034	0.020
2018Aug01-02	0.033	0.033	0.032	0.032	0.033	0.031	0.035	0.031
2018Aug13-01	0.035	0.034	0.036	0.036	0.037	0.036	0.038	0.034
2018Aug15-01	0.029	0.032	0.030	0.031	0.031	0.030	0.034	0.027
2018Aug16-01	0.022	0.022	0.020	0.022	0.020	0.020	0.024	0.022
2018Nov07-01	0.040	0.047	0.037	0.039	0.048	0.037	0.050	0.037
2018Nov09-02	0.032	0.051	0.049	0.050	0.050	0.048	0.047	0.030
Mean	0.025	0.027	0.026	0.027	0.028	0.025	0.031	0.024
SD	0.006	0.009	0.008	0.008	0.009	0.008	0.008	0.006

Table D.2 – Shoulder Horizontal Abduction Torque normalized (by body weight*height) results with mean and standard deviation (SD) for each specific inertial parameter changed. Coordinate system defined as follows: x is the medio-lateral axis, y is the longitudinal axis, and z is the anteroposterior axis.

	Inertial Parameter Changed							
Participant	***Segment Mass***	COM_x	COM_y	ROG_x	ROG_y	ROG_z	***All***	***None***
2017Jul19-01	0.056	0.053	0.049	0.053	0.052	0.053	0.046	0.053
2017Jul19-02	0.043	0.039	0.042	0.044	0.043	0.047	0.048	0.041
2017Jul21-01	0.041	0.041	0.046	0.048	0.046	0.053	0.059	0.041
2017Jul21-02	0.040	0.012	0.021	0.021	0.022	0.018	0.041	0.040
2017Jul26-01	0.044	0.033	0.034	0.041	0.039	0.039	0.043	0.042
2017Jul27-01	0.039	0.035	0.034	0.034	0.033	0.034	0.058	0.036
2017Jul27-02	0.034	0.015	0.034	0.034	0.034	0.034	0.047	0.032
2017Aug20-01	0.012	0.013	0.018	0.015	0.018	0.017	0.013	0.010
2017Aug20-02	0.027	0.028	0.028	0.028	0.030	0.030	0.035	0.027
2017Aug20-03	0.037	0.029	0.039	0.040	0.039	0.042	0.061	0.033
2017Sep07-02	0.038	0.030	0.057	0.057	0.055	0.060	0.055	0.036
2017Sep30-01	0.058	0.039	0.054	0.057	0.055	0.058	0.083	0.057
2018Aug01-02	0.024	0.041	0.034	0.030	0.031	0.031	0.040	0.024
2018Aug13-01	0.076	0.077	0.063	0.063	0.063	0.063	0.076	0.075
2018Aug15-01	0.071	0.069	0.077	0.065	0.068	0.066	0.072	0.067
2018Aug16-01	0.054	0.033	0.042	0.033	0.042	0.030	0.072	0.058
2018Nov07-01	0.093	0.096	0.098	0.119	0.117	0.117	0.147	0.088
2018Nov09-02	0.073	0.084	0.085	0.074	0.077	0.076	0.120	0.067
Mean	0.048	0.043	0.047	0.048	0.048	0.048	0.062	0.046
SD	0.020	0.024	0.021	0.023	0.023	0.023	0.030	0.019

Table D.3 – Shoulder Compression Force normalized (by body weight) results with mean and standard deviation (SD) for each specific inertial parameter changed. Coordinate system defined as follows: x is the medio-lateral axis, y is the longitudinal axis, and z is the anteroposterior axis.

	Inertial Parameter Changed							
Participant	***Segment Mass***	COM_x	COM_y	ROG_x	ROG_y	ROG_z	***All***	***None***
2017Jul19-01	0.497	0.539	0.511	0.522	0.522	0.522	0.559	0.482
2017Jul19-02	0.734	0.833	0.780	0.807	0.807	0.807	0.776	0.690
2017Jul21-01	0.526	0.613	0.552	0.569	0.569	0.569	0.569	0.519
2017Jul21-02	0.550	0.561	0.532	0.532	0.532	0.518	0.573	0.525
2017Jul26-01	0.721	0.732	0.679	0.696	0.696	0.696	0.732	0.679
2017Jul27-01	0.584	0.574	0.543	0.551	0.551	0.551	0.657	0.538
2017Jul27-02	0.583	0.569	0.561	0.579	0.579	0.579	0.575	0.563
2017Aug20-01	0.522	0.561	0.521	0.531	0.531	0.531	0.568	0.515
2017Aug20-02	0.583	0.543	0.543	0.543	0.543	0.543	0.626	0.594
2017Aug20-03	0.702	0.711	0.634	0.661	0.661	0.661	0.780	0.612
2017Sep07-02	0.615	0.736	0.676	0.696	0.696	0.696	0.696	0.579
2017Sep30-01	0.636	0.549	0.534	0.550	0.550	0.550	0.595	0.574
2018Aug01-02	0.819	0.718	0.664	0.672	0.672	0.672	0.888	0.754
2018Aug13-01	0.708	0.763	0.749	0.749	0.749	0.749	0.708	0.707
2018Aug15-01	0.789	0.843	0.803	0.812	0.812	0.812	0.824	0.739
2018Aug16-01	0.588	0.557	0.526	0.557	0.526	0.529	0.599	0.586
2018Nov07-01	0.766	0.728	0.592	0.631	0.631	0.631	0.847	0.725
2018Nov09-02	0.852	1.020	0.950	0.961	0.961	0.961	1.040	0.762
Mean	0.654	0.675	0.631	0.646	0.644	0.643	0.701	0.619
SD	0.106	0.131	0.119	0.120	0.121	0.122	0.133	0.090

Table D.4 – Elbow Varus Torque normalized (by body weight*height) results with mean and standard deviation (SD) for each specific inertial parameter changed. Coordinate system defined as follows: x is the medio-lateral axis, y is the longitudinal axis, and z is the anteroposterior axis.

	Inertial Parameter Changed							
Participant	***Segment Mass***	COM_x	COM_y	ROG_x	ROG_y	ROG_z	***All***	***None***
2017Jul19-01	0.018	0.018	0.018	0.018	0.018	0.018	0.018	0.017
2017Jul19-02	0.021	0.022	0.022	0.022	0.022	0.022	0.022	0.020
2017Jul21-01	0.016	0.016	0.016	0.016	0.016	0.016	0.016	0.016
2017Jul21-02	0.024	0.024	0.024	0.024	0.024	0.024	0.024	0.024
2017Jul26-01	0.025	0.031	0.031	0.031	0.031	0.031	0.030	0.024
2017Jul27-01	0.014	0.015	0.015	0.015	0.015	0.014	0.014	0.014
2017Jul27-02	0.020	0.019	0.019	0.019	0.019	0.019	0.019	0.020
2017Aug20-01	0.020	0.020	0.020	0.020	0.020	0.020	0.019	0.020
2017Aug20-02	0.016	0.014	0.014	0.014	0.014	0.014	0.017	0.016
2017Aug20-03	0.017	0.016	0.016	0.016	0.016	0.016	0.017	0.016
2017Sep07-02	0.023	0.023	0.023	0.023	0.023	0.023	0.023	0.022
2017Sep30-01	0.016	0.016	0.016	0.016	0.016	0.016	0.016	0.017
2018Aug01-02	0.024	0.022	0.022	0.022	0.022	0.022	0.025	0.023
2018Aug13-01	0.028	0.028	0.029	0.029	0.029	0.029	0.031	0.028
2018Aug15-01	0.025	0.023	0.023	0.023	0.023	0.023	0.023	0.023
2018Aug16-01	0.018	0.011	0.011	0.011	0.011	0.011	0.017	0.019
2018Nov07-01	0.018	0.013	0.013	0.013	0.013	0.013	0.019	0.019
2018Nov09-02	0.020	0.038	0.038	0.038	0.038	0.038	0.022	0.020
Mean	0.020	0.021	0.021	0.021	0.021	0.021	0.021	0.020
SD	0.004	0.007	0.007	0.007	0.007	0.007	0.005	0.003

APPENDIX E: Body Fat Percentage/Body Mass vs Kinetic Predictions - Regression Results

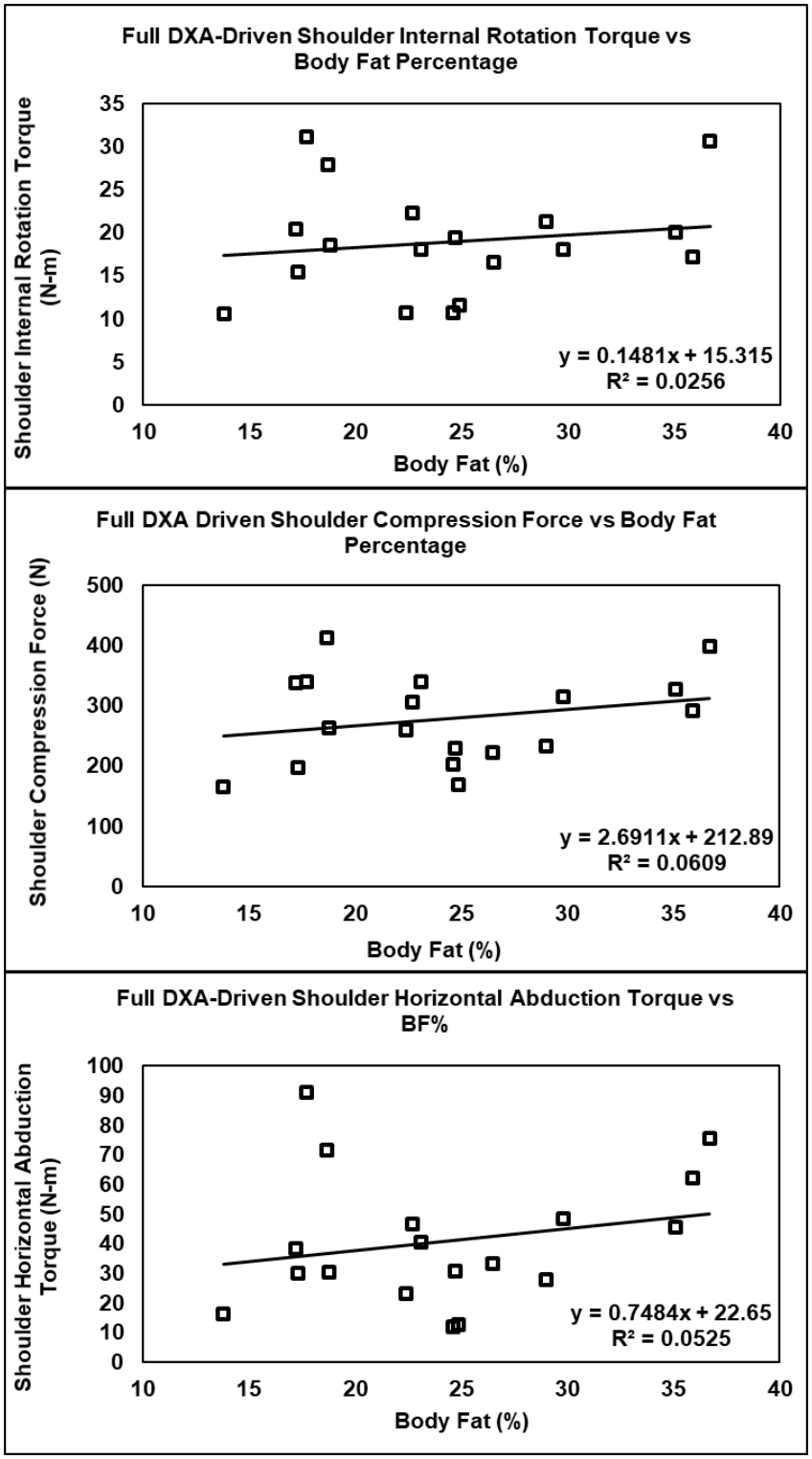

Figure E.1: Regression plots for full DXA-driven shoulder results against body fat percentage. *Note:* R^2 results presented on plots are with body fat percentage as the independent variable and the shoulder kinetic parameter as the dependent value.

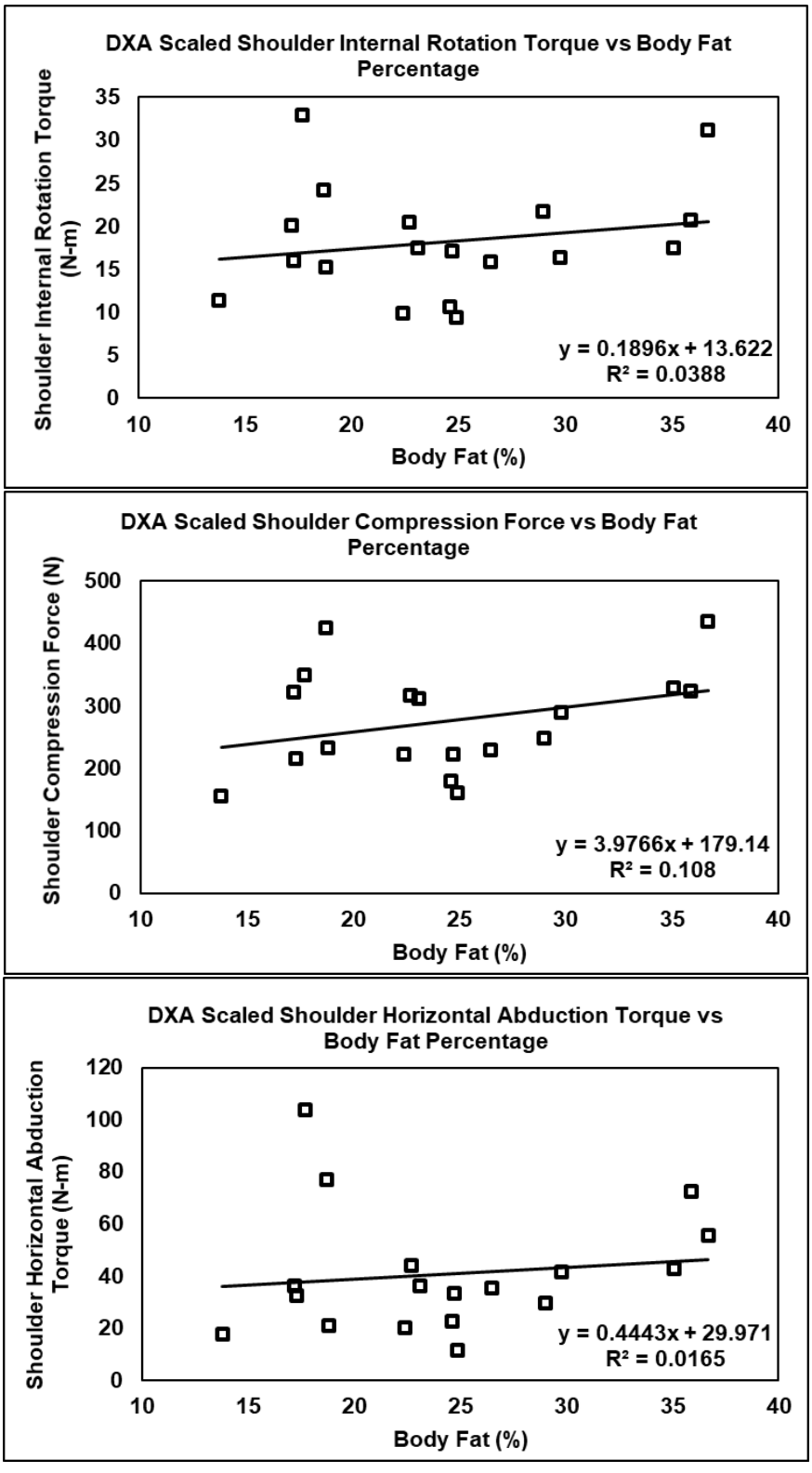

Figure E.2: Regression plots for DXA scaled shoulder results against body fat percentage. *Note:* R^2 results presented on plots are with body fat percentage as the independent variable and the shoulder kinetic parameter as the dependent value.

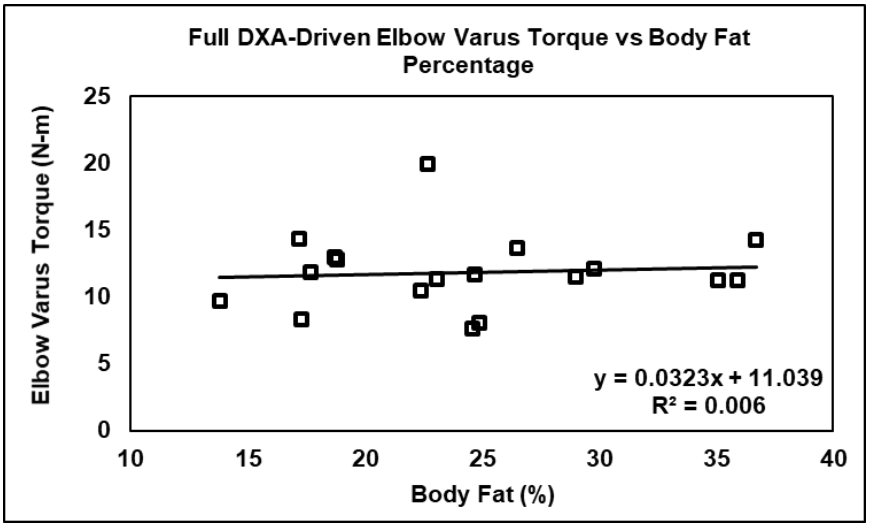

Figure E.3: Regression plot for full DXA-driven elbow varus torque against body fat percentage. *Note:* R^2 results presented on plots are with body fat percentage as the independent variable and the shoulder kinetic parameter as the dependent value.

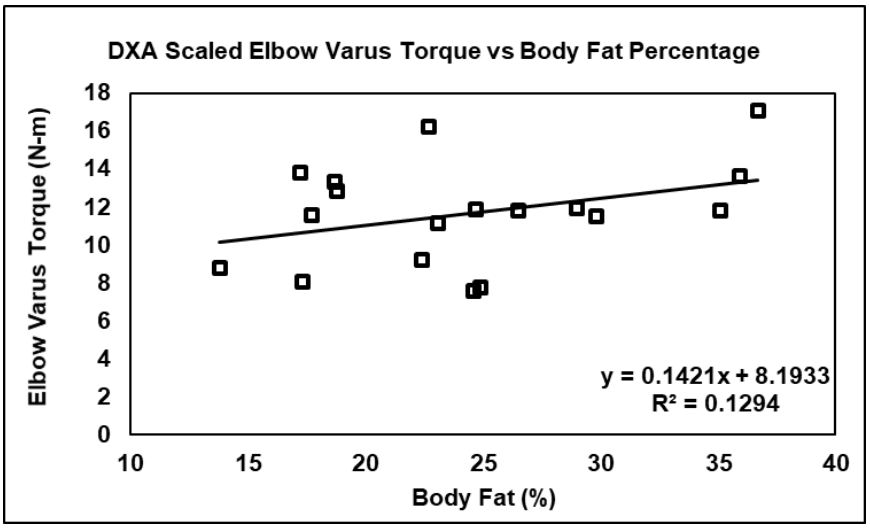

Figure E.4: Regression plot for DXA Scaled elbow varus torque against body fat percentage. *Note:* R^2 results presented on plots are with body fat percentage as the independent variable and the shoulder kinetic parameter as the dependent value.

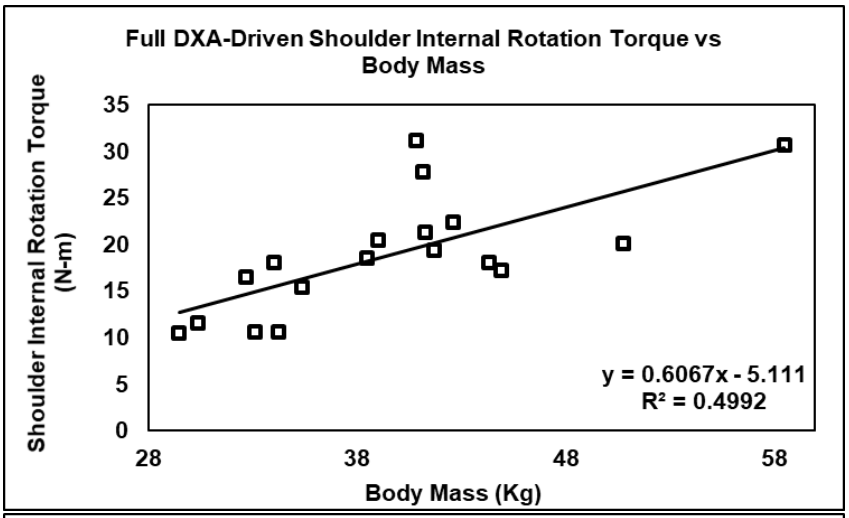

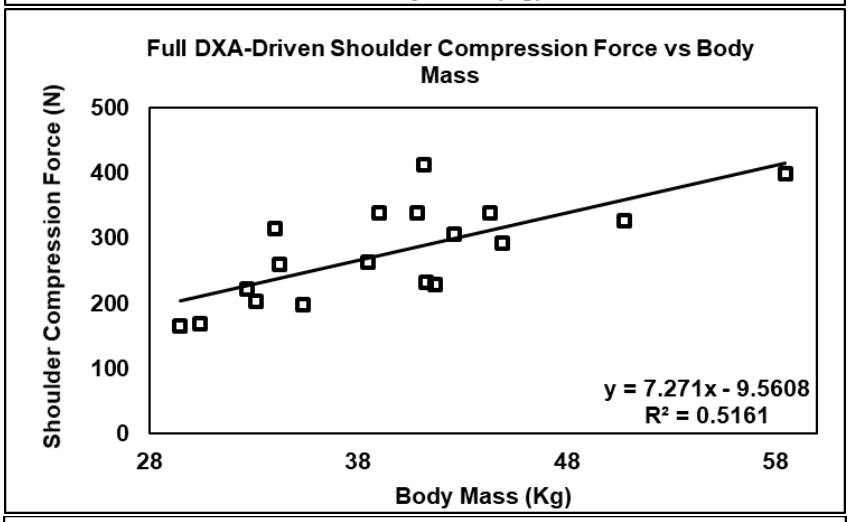

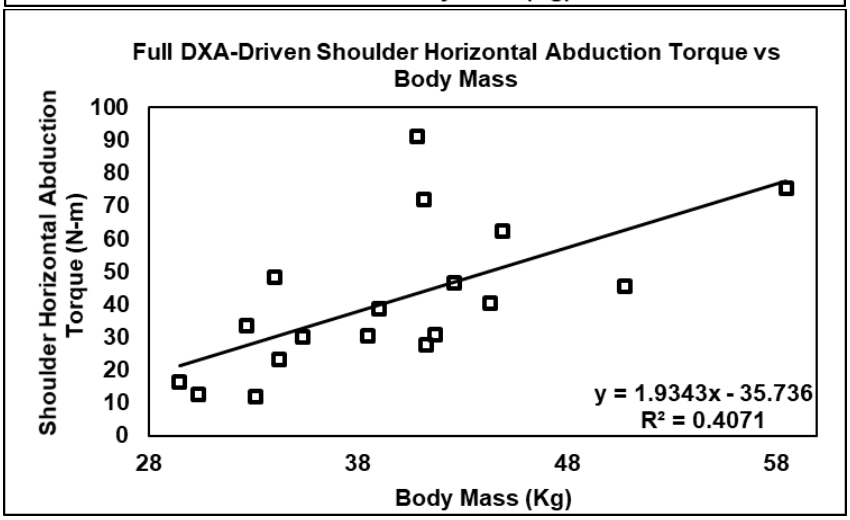

Figure E.5: Regression plots for full DXA-driven shoulder results against body mass. *Note:* R^2 results presented on plots are with body mass as the independent variable and the shoulder kinetic parameter as the dependent value.

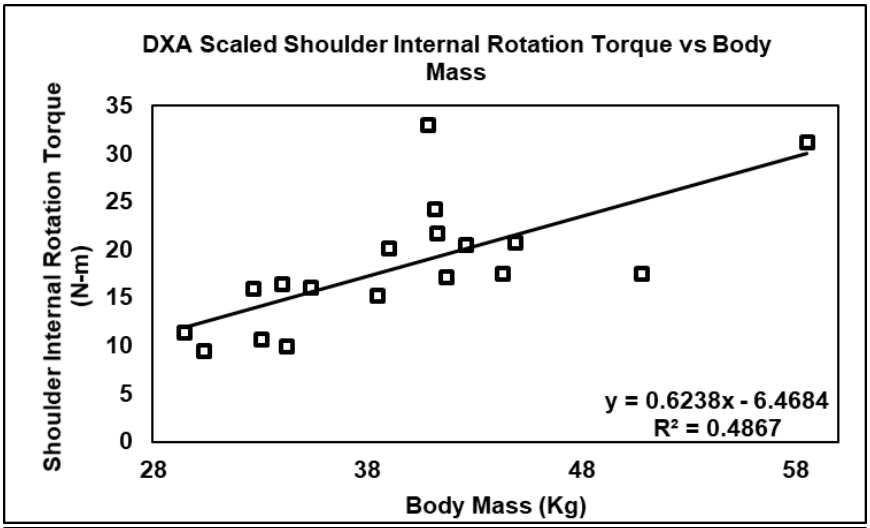

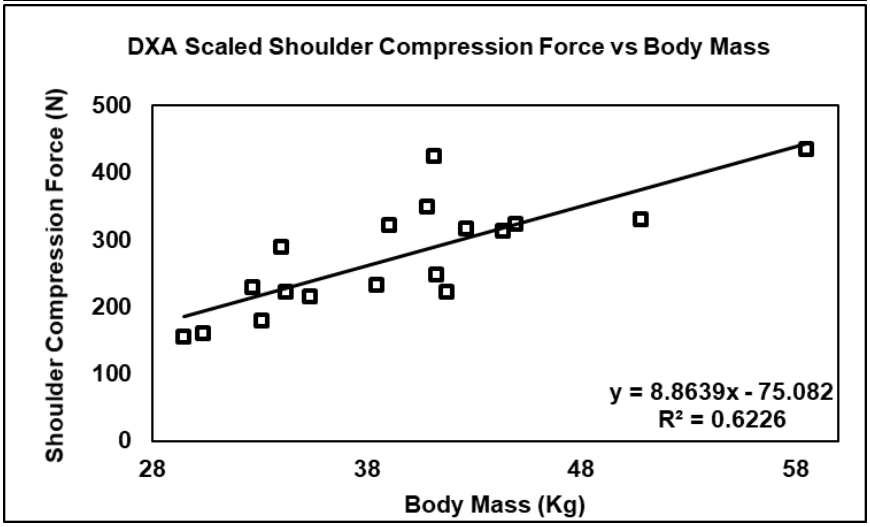

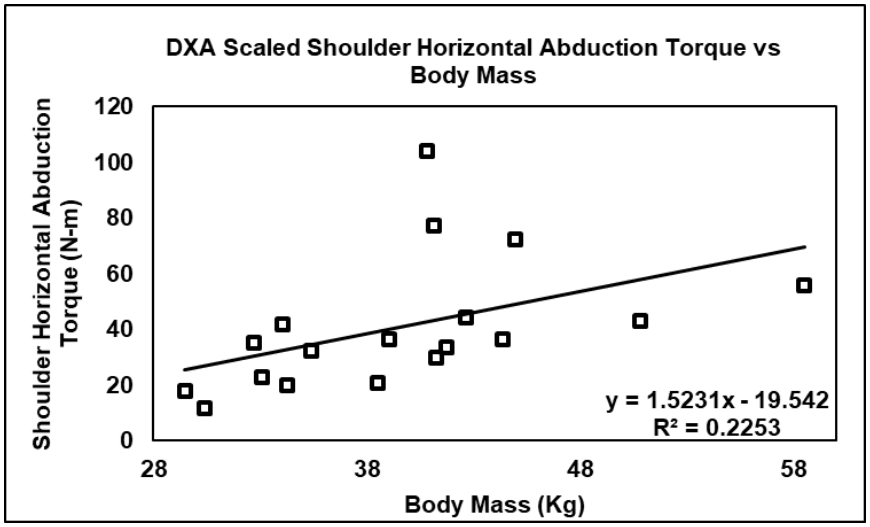

Figure E.6: Regression plots for DXA scaled shoulder results against body mass. *Note:* R^2 results presented on plots are with body mass as the independent variable and the shoulder kinetic parameter as the dependent value.

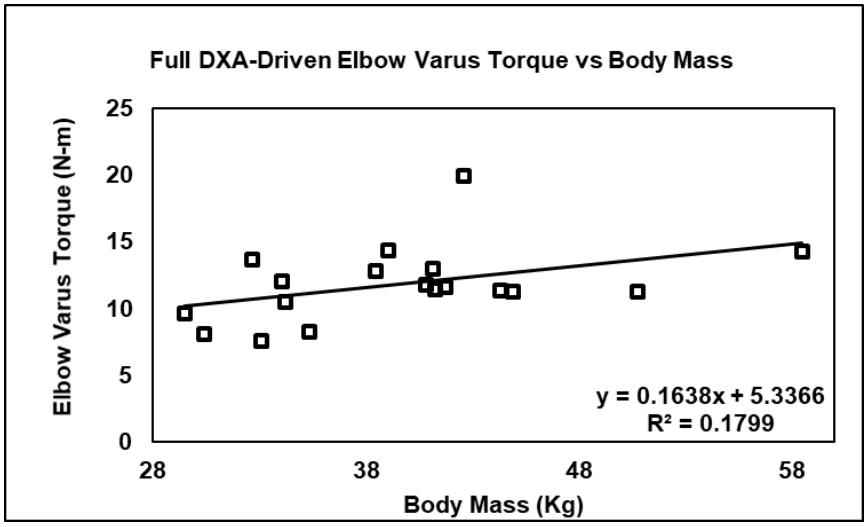

Figure E.7: Regression plot for full DXA-driven elbow varus torque against body mass. *Note:* R^2 results presented on plots are with body mass as the independent variable and the shoulder kinetic parameter as the dependent value.

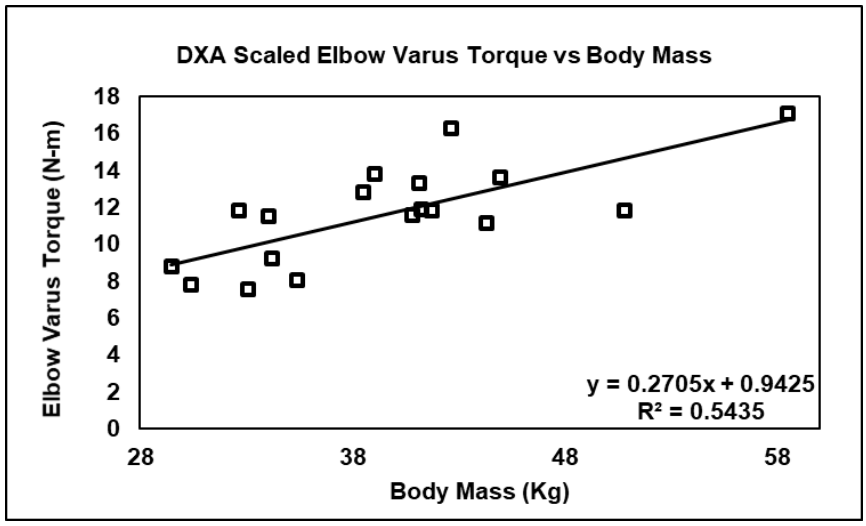

Figure E.8: Regression plot for DXA Scaled elbow varus torque against body mass. *Note:* R^2 results presented on plots are with body mass as the independent variable and the shoulder kinetic parameter as the dependent value.

APPENDIX F: Segment Mass Index (SMI) Power Investigation

The segment mass index equation (Equation F-1) was investigated similar to the development of the equation that represents body mass index (Equation F-2).

$$Segment\ Mass\ Index = \frac{M_{segment(s)}}{L_{segment(s)}{}^{p}} \quad \text{(F-1)}$$

$$Body\ Mass\ Index = \frac{M_{body}}{H_{body}{}^{p}} \quad \text{(F-2)}$$

Where the power, p, is changed and optimized via linear regression analysis in a logarithmic manner. While the power for BMI is commonly debated to be between 1 and 2, the logarithmic linear regression lies closer to 2 (approximately 1.7). As a result, many widely used versions of the BMI formulae are seen to carry a power of 2.

The logarithmic approach is as follows; first, the segment(s) mass,m, is assumed to be proportional, via a constant b, to the segment(s) length, l, raised to the power, p (Equation F-3).

$$m = b * l^{p} \quad \text{(F-3)}$$

The log is then taken of both sides. Using log rules, the equation is simplified, resulting in the equation of a line (Equation F-4).

$$\log(m) = \log(b) + p * \log(l) \quad \text{(F-4)}$$

A best fit linear regression to $\log(m)$ vs $\log(l)$ then gives us a y-intercept, $\log(b)$, and a slope, p. Thus, one can achieve the power for their data and, in theory, get a better formula to use.

For this study, SMI power was investigated for the total arm (hand, forearm, and upper arm) and lower arm (hand and forearm) because the inverse dynamic analysis at the joints of interest (shoulder and elbow) only depend on segments on the distal end of the joint. For the total arm (Figure F.1A), the logarithmic analysis resulted in a power of 1.69. For the lower arm (Figure F.1B), the logarithmic analysis resulted in a power of 1.57.

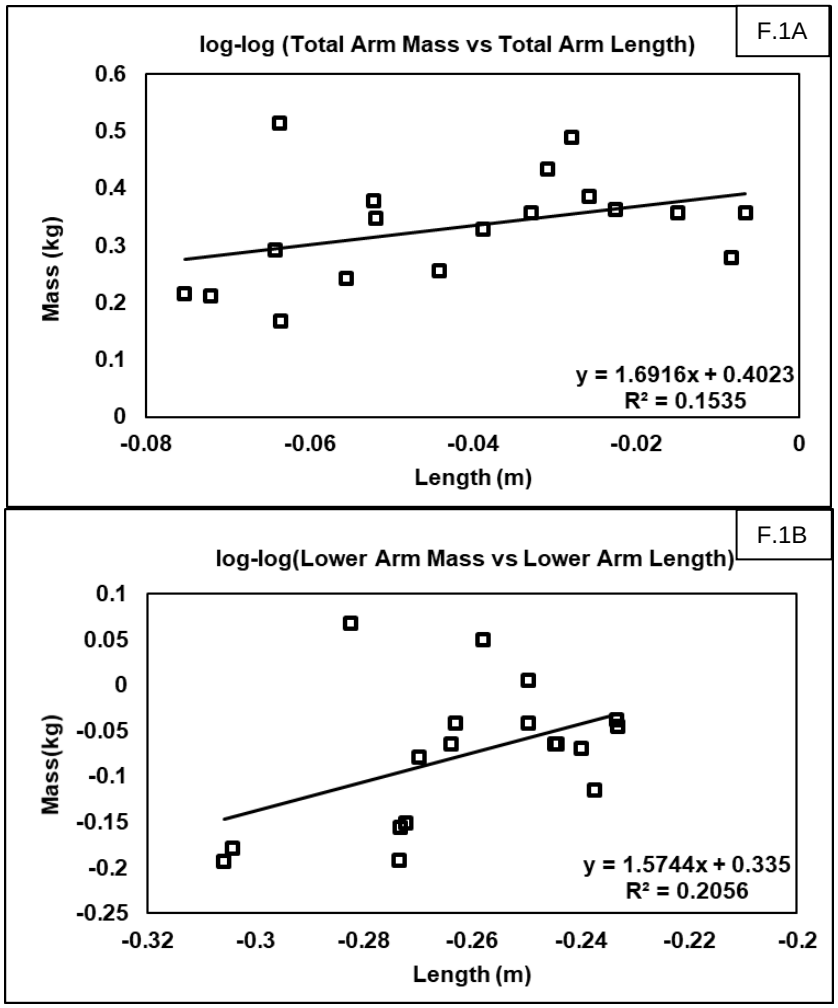

Figure F.1: Logarithmic plots. F.1A) Total arm mass vs total arm length for all 18 participants. F.1B) Lower arm mass vs lower arm length for all 18 participants.

Using these powers, four linear regressions were performed: between the 3 full DXA-driven shoulder kinetics and total arm SMI, with the p value of 1.69 (Figures F.2 – F.4), and between full DXA-driven EVT and lower arm SMI, with the p-value of 1.57 (Figure F.5).

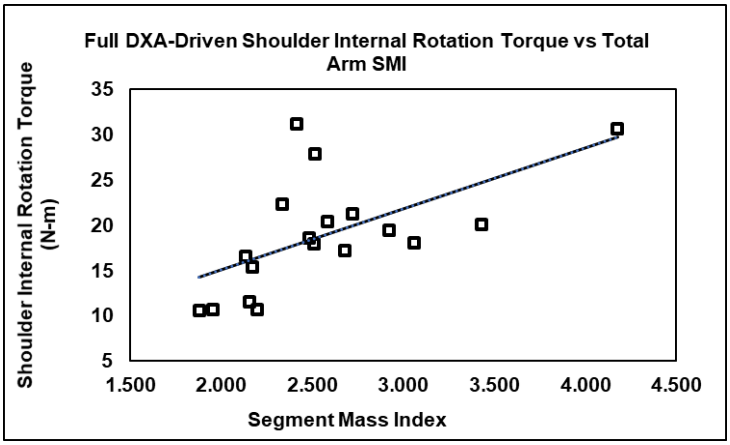

Regression Analysis: SIRT versus Total Arm SMI -p

Analysis of Variance

Source	DF	Adj SS	Adj MS	F-Value	P-Value
Regression	1	243.5	243.51	9.10	0.008
Total Arm SMI -p	1	243.5	243.51	9.10	0.008
Error	16	428.0	26.75		
Total	17	671.5			

Model Summary

S	R-sq	R-sq(adj)	R-sq(pred)
5.17201	36.26%	32.28%	24.52%

Coefficients

Term	Coef	SE Coef	T-Value	P-Value	VIF
Constant	1.51	5.90	0.26	0.801	
Total Arm SMI -p	6.76	2.24	3.02	0.008	1.00

Regression Equation

SIRT = 1.51 + 6.76 Total Arm SMI -p

Fits and Diagnostics for Unusual Observations

Obs	SIRT	Fit	Resid	Std Resid	
12	30.64	29.77	0.87	0.25	X
17	31.19	17.84	13.35	2.66	R

R Large residual
X Unusual X

Figure F.2: Linear regression plot and statistics for full DXA-driven SIRT vs Total Arm SMI. A power value of 1.69 was used in the SMI formula. *Note:* This analysis was done as a side investigation. There were no conclusions from these statistical results.

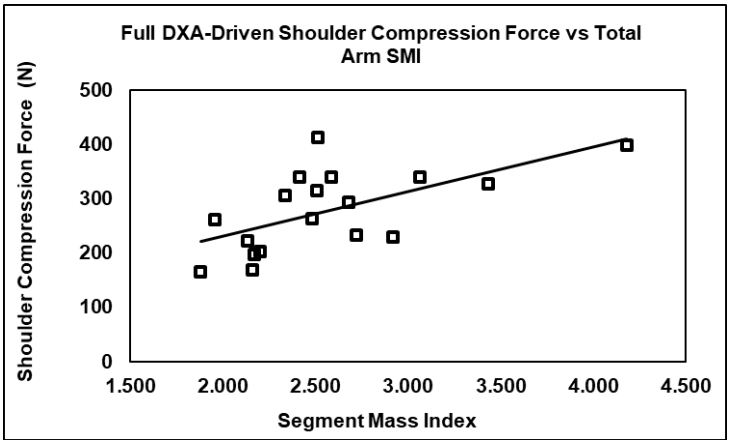

Regression Analysis: SCF versus Total Arm SMI -p

Analysis of Variance

Source	DF	Adj SS	Adj MS	F-Value	P-Value
Regression	1	36020	36020	10.06	0.006
Total Arm SMI -p	1	36020	36020	10.06	0.006
Error	16	57271	3579		
Total	17	93291			

Model Summary

S	R-sq	R-sq(adj)	R-sq(pred)
59.8285	38.61%	34.77%	27.95%

Coefficients

Term	Coef	SE Coef	T-Value	P-Value	VIF
Constant	66.7	68.2	0.98	0.343	
Total Arm SMI -p	82.2	25.9	3.17	0.006	1.00

Regression Equation

SCF = 66.7 + 82.2 Total Arm SMI -p

Fits and Diagnostics for Unusual Observations

Obs	SCF	Fit	Resid	Std Resid	
12	399.0	410.4	-11.4	-0.28	X
18	412.3	273.7	138.6	2.38	R

R Large residual
X Unusual X

Figure F.3: Linear regression plot and statistics for full DXA-driven SCF vs Total Arm SMI. A power value of 1.69 was used in the SMI formula. *Note:* This analysis was done as a side investigation. There were no conclusions from these statistical results.

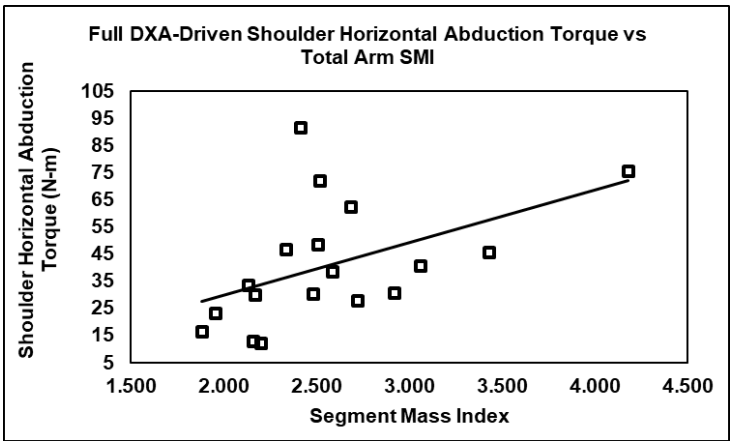

Regression Analysis: SHAT versus Total Arm SMI -p

Analysis of Variance

Source	DF	Adj SS	Adj MS	F-Value	P-Value
Regression	1	2005	2005.5	5.04	0.039
Total Arm SMI -p	1	2005	2005.5	5.04	0.039
Error	16	6364	397.8		
Total	17	8370			

Model Summary

S	R-sq	R-sq(adj)	R-sq(pred)
19.9440	23.96%	19.21%	11.47%

Coefficients

Term	Coef	SE Coef	T-Value	P-Value	VIF
Constant	-9.1	22.7	-0.40	0.695	
Total Arm SMI -p	19.41	8.64	2.25	0.039	1.00

Regression Equation

SHAT = -9.1 + 19.41 Total Arm SMI -p

Fits and Diagnostics for Unusual Observations

Obs	SHAT	Fit	Resid	Std Resid	
12	75.51	72.01	3.50	0.26	X
17	91.23	37.78	53.45	2.76	R

R Large residual
X Unusual X

Figure F.4: Linear regression plot and statistics for full DXA-driven SHAT vs Total Arm SMI. A power value of 1.69 was used in the SMI formula. *Note:* This analysis was done as a side investigation. There were no conclusions from these statistical results.

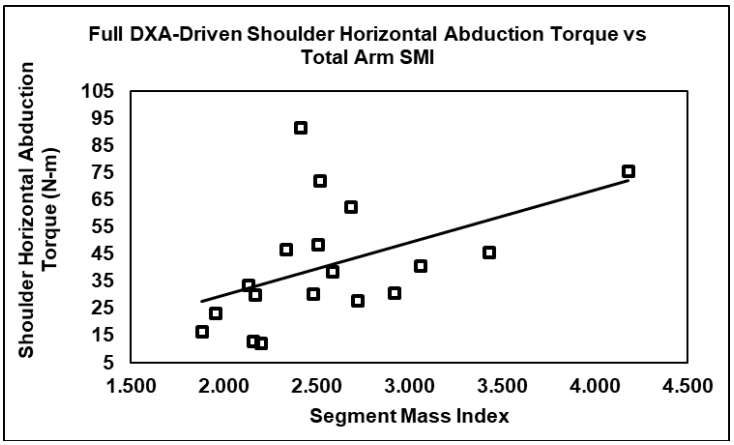

Regression Analysis: EVT versus Lower Arm SMI - p

Analysis of Variance

Source	DF	Adj SS	Adj MS	F-Value	P-Value
Regression	1	9.732	9.732	1.23	0.283
Lower Arm SMI - p	1	9.732	9.732	1.23	0.283
Error	16	126.122	7.883		
Total	17	135.855			

Model Summary

S	R-sq	R-sq(adj)	R-sq(pred)
2.80761	7.16%	1.36%	0.00%

Coefficients

Term	Coef	SE Coef	T-Value	P-Value	VIF
Constant	7.41	4.03	1.84	0.084	
Lower Arm SMI - p	2.02	1.81	1.11	0.283	1.00

Regression Equation

EVT = 7.41 + 2.02 Lower Arm SMI - p

Fits and Diagnostics for Unusual Observations

Obs	EVT	Fit	Resid	Std Resid	
5	19.94	11.64	8.30	3.05	R
12	14.26	13.98	0.29	0.15	X

R Large residual
X Unusual X

Figure F.5: Linear regression plot and statistics for full DXA-driven EVT vs Lower Arm SMI. A power value of 1.57 was used in the SMI formula. *Note:* This analysis was done as a side investigation. There were no conclusions from these statistical results.

In addition, further regression analysis was completed to obtain p-values and coefficients of determination (R^2) values by comparing segment mass index results from powers of 1, 2, or 3 and full DXA-driven kinetic predictions. (Table F.1)

Table F.1 – Linear regression results for full DXA-driven kinetic predictions vs segment mass index.

	SMI Formula Power (p)	**P-Value**	**R^2**
SIRT	1	0.003	.418
	1.69	0.008	.362
	2	0.012	.335
	3	0.038	.242
SCF	1	0.002	.477
	1.69	0.006	.386
	2	0.010	.344
	3	0.051	.218
SHAT	1	0.018	.305
	1.69	0.039	.240
	2	0.055	.211
	3	0.148	.126
EVT	1	0.145	.127
	1.57	0.283	.072
	2	0.430	.039
	3	0.868	.001

APPENDIX G: Full DXA-driven Segment Mass Association Results

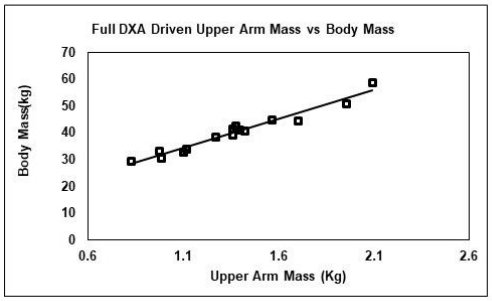

Regression Analysis: Body Mass versus Upper Arm Mass

Analysis of Variance

Source	DF	Adj SS	Adj MS	F-Value	P-Value
Regression	1	866.46	866.464	313.47	0.000
Upper Arm Mass	1	866.46	866.464	313.47	0.000
Error	16	44.23	2.764		
Total	17	910.69			

Model Summary

S	R-sq	R-sq(adj)	R-sq(pred)
1.66255	95.14%	94.84%	92.71%

Coefficients

Term	Coef	SE Coef	T-Value	P-Value	VIF
Constant	11.10	1.66	6.70	0.000	
Upper Arm Mass	21.23	1.20	17.71	0.000	1.00

Regression Equation

Body Mass = 11.10 + 21.23 Upper Arm Mass

Fits and Diagnostics for Unusual Observations

Obs	Body Mass	Fit	Resid	Std Resid		
12	58.513	55.515	2.998	2.23	R	X

R Large residual
X Unusual X

Figure G.1: Linear regression plot and statistics for full DXA-driven Upper Arm Mass vs Body Mass. *Note:* This analysis was done as a side investigation. There were no conclusions drawn from these statistical results.

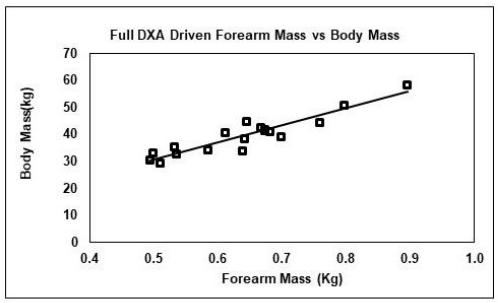

Regression Analysis: Body Mass versus Forearm Mass

Analysis of Variance

Source	DF	Adj SS	Adj MS	F-Value	P-Value
Regression	1	787.5	787.477	102.26	0.000
Forearm Mass	1	787.5	787.477	102.26	0.000
Error	16	123.2	7.701		
Total	17	910.7			

Model Summary

S	R-sq	R-sq(adj)	R-sq(pred)
2.77503	86.47%	85.62%	82.81%

Coefficients

Term	Coef	SE Coef	T-Value	P-Value	VIF
Constant	2.27	3.75	0.61	0.553	
Forearm Mass	63.24	6.25	10.11	0.000	1.00

Regression Equation

Body Mass = 2.27 + 63.24 Forearm Mass

Fits and Diagnostics for Unusual Observations

Obs	Body Mass	Fit	Resid	Std Resid	
12	58.51	55.75	2.76	1.27	X
15	34.05	39.46	-5.41	-2.00	R

R Large residual
X Unusual X

Figure G.2: Linear regression plot and statistics for full DXA-driven Forearm Mass vs Body Mass. *Note:* This analysis was done as a side investigation. There were no conclusions drawn from these statistical results.

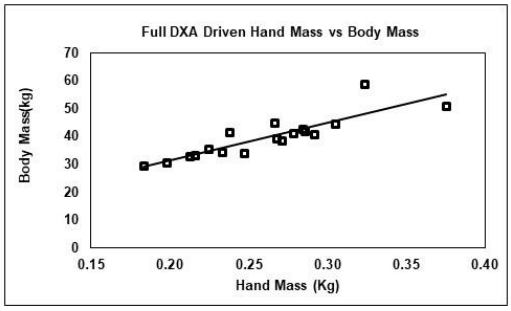

Regression Analysis: Body Mass versus Hand Mass

Analysis of Variance

Source	DF	Adj SS	Adj MS	F-Value	P-Value
Regression	1	702.3	702.29	53.92	0.000
Hand Mass	1	702.3	702.29	53.92	0.000
Error	16	208.4	13.02		
Total	17	910.7			

Model Summary

S	R-sq	R-sq(adj)	R-sq(pred)
3.60897	77.12%	75.69%	67.65%

Coefficients

Term	Coef	SE Coef	T-Value	P-Value	VIF
Constant	4.32	4.88	0.89	0.389	
Hand Mass	135.0	18.4	7.34	0.000	1.00

Regression Equation

Body Mass = 4.32 + 135.0 Hand Mass

Fits and Diagnostics for Unusual Observations

Obs	Body Mass	Fit	Resid	Std Resid	
6	50.80	54.98	-4.18	-1.49	X
12	58.51	48.04	10.47	3.16	R

R Large residual
X Unusual X

Figure G.3: Linear regression plot and statistics for full DXA-driven Hand Mass vs Body Mass. *Note:* This analysis was done as a side investigation. There were no conclusions drawn from these statistical results.

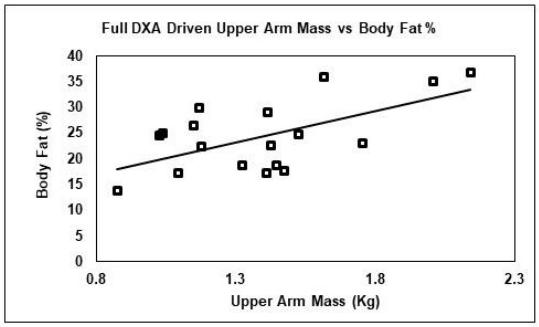

Regression Analysis: Body Fat % versus Upper Arm Mass

Analysis of Variance

Source	DF	Adj SS	Adj MS	F-Value	P-Value
Regression	1	285.8	285.77	9.16	0.008
Upper Arm Mass	1	285.8	285.77	9.16	0.008
Error	16	499.3	31.21		
Total	17	785.1			

Model Summary

S	R-sq	R-sq(adj)	R-sq(pred)
5.58620	36.40%	32.43%	21.77%

Coefficients

Term	Coef	SE Coef	T-Value	P-Value	VIF
Constant	8.01	5.57	1.44	0.170	
Upper Arm Mass	12.19	4.03	3.03	0.008	1.00

Regression Equation

Body Fat % = 8.01 + 12.19 Upper Arm Mass

Fits and Diagnostics for Unusual Observations

Obs	Body Fat %	Fit	Resid	Std Resid	
12	36.70	33.51	3.19	0.71	X

X Unusual X

Figure G.4: Linear regression plot and statistics for full DXA-driven Upper Arm Mass vs Body Fat Percentage. *Note:* This analysis was done as a side investigation. There were no conclusions drawn from these statistical results.

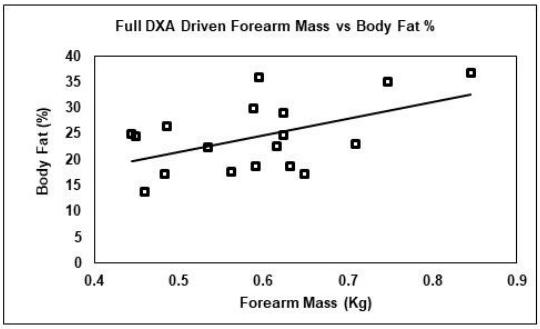

Regression Analysis: Body Fat % versus Forearm Mass

Analysis of Variance

Source	DF	Adj SS	Adj MS	F-Value	P-Value
Regression	1	201.5	201.53	5.53	0.032
Forearm Mass	1	201.5	201.53	5.53	0.032
Error	16	583.5	36.47		
Total	17	785.1			

Model Summary

S	R-sq	R-sq(adj)	R-sq(pred)
6.03910	25.67%	21.03%	6.54%

Coefficients

Term	Coef	SE Coef	T-Value	P-Value	VIF
Constant	5.49	8.16	0.67	0.511	
Forearm Mass	32.0	13.6	2.35	0.032	1.00

Regression Equation

Body Fat % = 5.49 + 32.0 Forearm Mass

Fits and Diagnostics for Unusual Observations

Obs	Body Fat %	Fit	Resid	Std Resid	
12	36.70	32.54	4.16	0.88	X

X Unusual X

Figure G.5: Linear regression plot and statistics for full DXA-driven Forearm Mass vs Body Fat Percentage. *Note:* This analysis was done as a side investigation. There were no conclusions drawn from these statistical results.

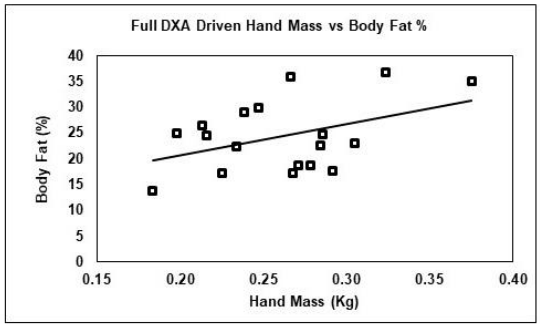

Regression Analysis: Body Fat % versus Hand Mass

Analysis of Variance

Source	DF	Adj SS	Adj MS	F-Value	P-Value
Regression	1	145.5	145.53	3.64	0.074
Hand Mass	1	145.5	145.53	3.64	0.074
Error	16	639.5	39.97		
Total	17	785.1			

Model Summary

S	R-sq	R-sq(adj)	R-sq(pred)
6.32224	18.54%	13.45%	0.00%

Coefficients

Term	Coef	SE Coef	T-Value	P-Value	VIF
Constant	8.32	8.55	0.97	0.345	
Hand Mass	61.5	32.2	1.91	0.074	1.00

Regression Equation

Body Fat % = 8.32 + 61.5 Hand Mass

Fits and Diagnostics for Unusual Observations

Obs	Body Fat %	Fit	Resid	Std Resid	
6	35.10	31.38	3.72	0.75	X

X Unusual X

Figure G.6: Linear regression plot and statistics for full DXA-driven Hand Mass vs Body Fat Percentage. *Note:* This analysis was done as a side investigation. There were no conclusions drawn from these statistical results.

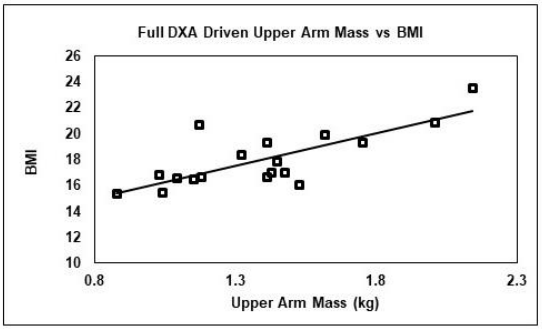

Regression Analysis: BMI versus Upper Arm Mass

Analysis of Variance

Source	DF	Adj SS	Adj MS	F-Value	P-Value
Regression	1	47.95	47.953	22.01	0.000
Upper Arm Mass	1	47.95	47.953	22.01	0.000
Error	16	34.86	2.179		
Total	17	82.81			

Model Summary

S	R-sq	R-sq(adj)	R-sq(pred)
1.47610	57.90%	55.27%	46.28%

Coefficients

Term	Coef	SE Coef	T-Value	P-Value	VIF
Constant	11.28	1.47	7.66	0.000	
Upper Arm Mass	5.00	1.06	4.69	0.000	1.00

Regression Equation

BMI = 11.28 + 5.00 Upper Arm Mass

Fits and Diagnostics for Unusual Observations

Obs	BMI	Fit	Resid	Std Resid	
12	23.518	21.723	1.795	1.51	X
15	20.726	16.869	3.857	2.73	R

R Large residual
X Unusual X

Figure G.7: Linear regression plot and statistics for full DXA-driven Upper Arm Mass vs BMI. *Note:* This analysis was done as a side investigation. There were no conclusions drawn from these statistical results.

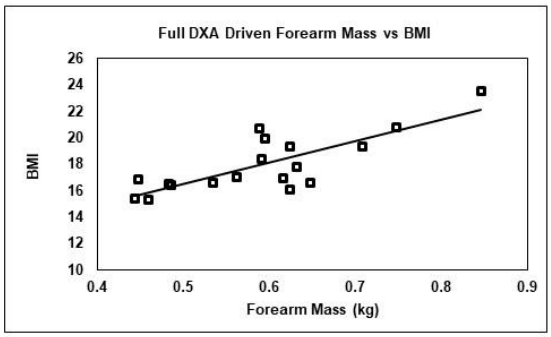

Regression Analysis: BMI versus Forearm Mass

Analysis of Variance

Source	DF	Adj SS	Adj MS	F-Value	P-Value
Regression	1	52.02	52.023	27.03	0.000
Forearm Mass	1	52.02	52.023	27.03	0.000
Error	16	30.79	1.924		
Total	17	82.81			

Model Summary

S	R-sq	R-sq(adj)	R-sq(pred)
1.38724	62.82%	60.50%	53.63%

Coefficients

Term	Coef	SE Coef	T-Value	P-Value	VIF
Constant	8.39	1.87	4.47	0.000	
Forearm Mass	16.25	3.13	5.20	0.000	1.00

Regression Equation

BMI = 8.39 + 16.25 Forearm Mass

Fits and Diagnostics for Unusual Observations

Obs	BMI	Fit	Resid	Std Resid	
12	23.518	22.129	1.389	1.28	X
15	20.726	17.942	2.784	2.07	R

R Large residual
X Unusual X

Figure G.8: Linear regression plot and statistics for full DXA-driven Forearm Mass vs Body Mass. *Note:* This analysis was done as a side investigation. There were no conclusions drawn from these statistical results.

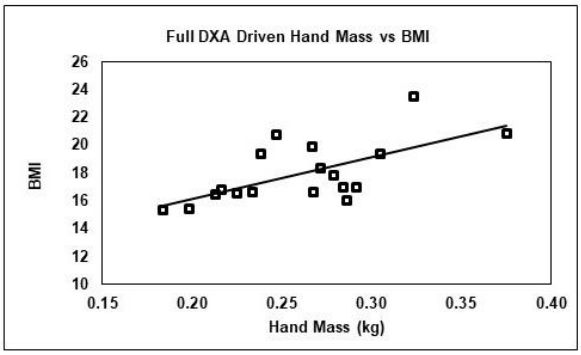

Regression Analysis: BMI versus Hand Mass

Analysis of Variance

Source	DF	Adj SS	Adj MS	F-Value	P-Value
Regression	1	34.06	34.060	11.18	0.004
Hand Mass	1	34.06	34.060	11.18	0.004
Error	16	48.75	3.047		
Total	17	82.81			

Model Summary

S	R-sq	R-sq(adj)	R-sq(pred)
1.74561	41.13%	37.45%	27.45%

Coefficients

Term	Coef	SE Coef	T-Value	P-Value	VIF
Constant	10.21	2.36	4.32	0.001	
Hand Mass	29.74	8.89	3.34	0.004	1.00

Regression Equation

BMI = 10.21 + 29.74 Hand Mass

Fits and Diagnostics for Unusual Observations

Obs	BMI	Fit	Resid	Std Resid	
6	20.819	21.367	-0.548	-0.40	X
12	23.518	19.838	3.680	2.30	R

R Large residual
X Unusual X

Figure G.9: Linear regression plot and statistics for full DXA-driven Hand Mass vs BMI. *Note:* This analysis was done as a side investigation. There were no conclusions drawn from these statistical results.

APPENDIX H: Statistical Summary of Kinetic Results

Repeated Measures ANOVA with Post-Hoc Tukey Test

General Linear Model: Shoulder Internal Rotation versus ... on Method

Method

Factor coding (-1, 0, +1)

Factor Information

Factor	Type	Levels	Values
Participants	Random	18	2017Aug20-01, 2017Aug20-02, 2017Aug20-03, 2017Jul19-01, 2017Jul19-02, 2017Jul21-01, 2017Jul21-02, 2017Jul26-01, 2017Jul27-01, 2017Jul27-02, 2017Sep07-02, 2017Sep30-01, 2018Aug01-02, 2018Aug13-01, 2018Aug15-01, 2018Aug16-01, 2018Nov07-01, 2018Nov09-02
Calculation Method	Fixed	4	DXA mass driven-Max, DXA Scaled - Max, Full DXA-driven -Max, Scaled-Max

Analysis of Variance

Source	DF	Adj SS	Adj MS	F-Value	P-Value
Participants	17	1793.1	105.479	21.35	0.000
Calculation Method	3	266.5	88.830	17.98	0.000
Error	51	252.0	4.941		
Total	71	2311.6			

Model Summary

S	R-sq	R-sq(adj)	R-sq(pred)
2.22282	89.10%	84.82%	78.27%

Coefficients

Term	Coef	SE Coef	T-Value	P-Value	VIF	
Constant	-16.694	0.262	-63.73	0.000		
Participants						
2017Aug20-01	7.14	1.08	6.61	0.000		*
2017Aug20-02	6.59	1.08	6.10	0.000		*
2017Aug20-03	-0.46	1.08	-0.42	0.675		*
2017Jul19-01	-0.18	1.08	-0.16	0.872		*
2017Jul19-02	6.61	1.08	6.12	0.000		*
2017Jul21-01	4.17	1.08	3.87	0.000		*
2017Jul21-02	6.79	1.08	6.29	0.000		*
2017Jul26-01	-1.81	1.08	-1.67	0.100		*
2017Jul27-01	0.11	1.08	0.10	0.919		*
2017Jul27-02	-1.01	1.08	-0.93	0.356		*
2017Sep07-02	1.20	1.08	1.11	0.272		*
2017Sep30-01	-7.87	1.08	-7.28	0.000		*
2018Aug01-02	-2.80	1.08	-2.59	0.012		*
2018Aug13-01	1.00	1.08	0.93	0.358		*
2018Aug15-01	0.68	1.08	0.63	0.529		*
2018Aug16-01	-3.27	1.08	-3.03	0.004		*
2018Nov07-01	-11.24	1.08	-10.41	0.000		*
Calculation Method						
DXA mass driven-Max	1.531	0.454	3.37	0.001	1.50	
DXA Scaled - Max	-1.551	0.454	-3.42	0.001	1.50	
Full DXA-driven -Max	-2.232	0.454	-4.92	0.000	1.50	

Regression Equation

Shoulder Internal Rotation = -16.694 + 7.14 Participants_2017Aug20-01 + 6.59 Participants_2017Aug20-02 - 0.46 Participants_2017Aug20-03 - 0.18 Participants_2017Jul19-01 + 6.61 Participants_2017Jul19-02 + 4.17 Participants_2017Jul21-01 + 6.79 Participants_2017Jul21-02 - 1.81 Participants_2017Jul26-01 + 0.11 Participants_2017Jul27-01 - 1.01 Participants_2017Jul27-02 + 1.20 Participants_2017Sep07-02 - 7.87 Participants_2017Sep30-01 - 2.80 Participants_2018Aug01-02 + 1.00 Participants_2018Aug13-01 + 0.68 Participants_2018Aug15-01 - 3.27 Participants_2018Aug16-01 - 11.24 Participants_2018Nov07-01 - 5.68 Participants_2018Nov09-02 + 1.531 Calculation Method_DXA mass driven-Max - 1.551 Calculation Method_DXA Scaled - Max - 2.232 Calculation Method_Full DXA-driven -Max + 2.252 Calculation Method_Scaled-Max

Equation treats random terms as though they are fixed.

Fits and Diagnostics for Unusual Observations

Obs	Shoulder Internal Rotation	Fit	Resid	Std Resid	
45	-17.66	-22.31	4.65	2.48	R
46	-18.70	-23.03	4.32	2.31	R
47	-30.64	-26.79	-3.84	-2.06	R
48	-31.24	-26.11	-5.13	-2.74	R
63	-17.26	-22.19	4.93	2.64	R

R Large residual

Expected Mean Squares, using Adjusted SS

	Source	Expected Mean Square for Each Term
1	Participants	(3) + 4.0000 (1)
2	Calculation Method	(3) + Q[2]
3	Error	(3)

Error Terms for Tests, using Adjusted SS

	Source	Error DF	Error MS	Synthesis of Error MS
1	Participants	51.00	4.9409	(3)
2	Calculation Method	51.00	4.9409	(3)

Variance Components, using Adjusted SS

Source	Variance	% of Total	StDev	% of Total
Participants	25.1345	83.57%	5.01343	91.42%
Error	4.94093	16.43%	2.22282	40.53%
Total	30.0755		5.48411	

Comparisons for Shoulder Internal Rotation

Tukey Pairwise Comparisons: Calculation Method

Grouping Information Using the Tukey Method and 95% Confidence

Calculation Method	N	Mean	Grouping	
Scaled-Max	18	-14.4419	A	
DXA mass driven-Max	18	-15.1630	A	
DXA Scaled - Max	18	-18.2453		B
Full DXA-driven -Max	18	-18.9261		B

Means that do not share a letter are significantly different.

Tukey Simultaneous Tests for Differences of Means

Difference of Calculation Method Levels	Difference of Means	SE of Difference	Simultaneous 95% CI	T-Value
DXA Scaled - Max - DXA mass driven-Max	-3.082	0.741	(-5.052, -1.112)	-4.16
Full DXA-driven -Max - DXA mass driven-Max	-3.763	0.741	(-5.733, -1.793)	-5.08
Scaled-Max - DXA mass driven-Max	0.721	0.741	(-1.249, 2.691)	0.97
Full DXA-driven -Max - DXA Scaled - Max	-0.681	0.741	(-2.651, 1.289)	-0.92
Scaled-Max - DXA Scaled - Max	3.803	0.741	(1.833, 5.773)	5.13
Scaled-Max - Full DXA-driven -Max	4.484	0.741	(2.514, 6.454)	6.05

Difference of Calculation Method Levels	Adjusted P-Value
DXA Scaled - Max - DXA mass driven-Max	0.001
Full DXA-driven -Max - DXA mass driven-Max	0.000
Scaled-Max - DXA mass driven-Max	0.765
Full DXA-driven -Max - DXA Scaled - Max	0.795
Scaled-Max - DXA Scaled - Max	0.000
Scaled-Max - Full DXA-driven -Max	0.000

Individual confidence level = 98.95%

Figure H.1: Repeated Measures ANOVA with Post-HOC Tukey results for Shoulder Internal Rotation Torque vs inverse dynamic calculation method. A Bonferroni correction factor of 4 was applied accordingly, leaving a significance level of p = 0.0125.

General Linear Model: Shoulder Horizontal Abduction ... ation Method

Method

Factor coding (-1, 0, +1)

Factor Information

Factor	Type	Levels	Values
Participants	Random	18	2017Aug20-01, 2017Aug20-02, 2017Aug20-03, 2017Jul19-01, 2017Jul19-02, 2017Jul21-01, 2017Jul21-02, 2017Jul26-01, 2017Jul27-01, 2017Jul27-02, 2017Sep07-02, 2017Sep30-01, 2018Aug01-02, 2018Aug13-01, 2018Aug15-01, 2018Aug16-01, 2018Nov07-01, 2018Nov09-02
Calculation Method	Fixed	4	DXA mass driven-Max, DXA Scaled - Max, Full DXA-driven -Max, Scaled-Max

Analysis of Variance

Source	DF	Adj SS	Adj MS	F-Value	P-Value
Participants	17	18922	1113.08	16.62	0.000
Calculation Method	3	2784	928.12	13.86	0.000
Error	51	3415	66.96		
Total	71	25122			

Model Summary

S	R-sq	R-sq(adj)	R-sq(pred)
8.18265	86.41%	81.08%	72.91%

Coefficients

Term	Coef	SE Coef	T-Value	P-Value	VIF	
Constant	34.650	0.964	35.93	0.000		
Participants						
2017Aug20-01	-23.34	3.98	-5.87	0.000		*
2017Aug20-02	-19.86	3.98	-4.99	0.000		*
2017Aug20-03	-3.93	3.98	-0.99	0.327		*
2017Jul19-01	-0.70	3.98	-0.17	0.862		*
2017Jul19-02	-13.67	3.98	-3.44	0.001		*
2017Jul21-01	-8.67	3.98	-2.18	0.034		*
2017Jul21-02	-18.10	3.98	-4.55	0.000		*
2017Jul26-01	2.92	3.98	0.74	0.465		*
2017Jul27-01	2.21	3.98	0.56	0.581		*
2017Jul27-02	-10.54	3.98	-2.65	0.011		*
2017Sep07-02	-11.71	3.98	-2.94	0.005		*
2017Sep30-01	15.39	3.98	3.87	0.000		*
2018Aug01-02	1.46	3.98	0.37	0.715		*
2018Aug13-01	-0.90	3.98	-0.23	0.821		*
2018Aug15-01	5.83	3.98	1.47	0.148		*
2018Aug16-01	17.96	3.98	4.52	0.000		*
2018Nov07-01	42.12	3.98	10.59	0.000		*
Calculation Method						
DXA mass driven-Max	-5.56	1.67	-3.33	0.002	1.50	
DXA Scaled - Max	6.15	1.67	3.68	0.001	1.50	
Full DXA-driven -Max	6.25	1.67	3.74	0.000	1.50	

Regression Equation

Shoulder Horizontal Abduction = 34.650 - 23.34 Participants_2017Aug20-01
- 19.86 Participants_2017Aug20-02
- 3.93 Participants_2017Aug20-03
- 0.70 Participants_2017Jul19-01
- 13.67 Participants_2017Jul19-02
- 8.67 Participants_2017Jul21-01
- 18.10 Participants_2017Jul21-02
+ 2.92 Participants_2017Jul26-01
+ 2.21 Participants_2017Jul27-01
- 10.54 Participants_2017Jul27-02
- 11.71 Participants_2017Sep07-02
+ 15.39 Participants_2017Sep30-01
+ 1.46 Participants_2018Aug01-02
- 0.90 Participants_2018Aug13-01
+ 5.83 Participants_2018Aug15-01
+ 17.96 Participants_2018Aug16-01
+ 42.12 Participants_2018Nov07-01
+ 23.52 Participants_2018Nov09-02
- 5.56 Calculation Method_DXA mass driven-Max
+ 6.15 Calculation Method_DXA Scaled - Max
+ 6.25 Calculation Method_Full DXA-driven -Max
- 6.85 Calculation Method_Scaled-Max

Equation treats random terms as though they are fixed.

Fits and Diagnostics for Unusual Observations

Obs	Shoulder Horizontal Abduction	Fit	Resid	Std Resid	
47	75.51	56.29	19.22	2.79	R
65	54.48	69.93	-15.44	-2.24	R
68	103.83	82.93	20.90	3.03	R

R Large residual

Expected Mean Squares, using Adjusted SS

	Source	Expected Mean Square for Each Term
1	Participants	(3) + 4.0000 (1)
2	Calculation Method	(3) + Q[2]
3	Error	(3)

Error Terms for Tests, using Adjusted SS

	Source	Error DF	Error MS	Synthesis of Error MS
1	Participants	51.00	66.9558	(3)
2	Calculation Method	51.00	66.9558	(3)

Variance Components, using Adjusted SS

Source	Variance	% of Total	StDev	% of Total
Participants	261.532	79.62%	16.1720	89.23%
Error	66.9558	20.38%	8.1827	45.15%
Total	328.488		18.1242	

Comparisons for Shoulder Horizontal Abduction

Tukey Pairwise Comparisons: Calculation Method

Grouping Information Using the Tukey Method and 95% Confidence

Calculation Method	N	Mean	Grouping	
Full DXA-driven -Max	18	40.8987	A	
DXA Scaled - Max	18	40.8045	A	
DXA mass driven-Max	18	29.0935		B
Scaled-Max	18	27.8025		B

Means that do not share a letter are significantly different.

Tukey Simultaneous Tests for Differences of Means

Difference of Calculation Method Levels	Difference of Means	SE of Difference	Simultaneous 95% CI	T-Value
DXA Scaled - Max - DXA mass driven-Max	11.71	2.73	(4.46, 18.96)	4.29
Full DXA-driven -Max - DXA mass driven-Max	11.81	2.73	(4.55, 19.06)	4.33
Scaled-Max - DXA mass driven-Max	-1.29	2.73	(-8.54, 5.96)	-0.47
Full DXA-driven -Max - DXA Scaled - Max	0.09	2.73	(-7.16, 7.35)	0.03
Scaled-Max - DXA Scaled - Max	-13.00	2.73	(-20.25, -5.75)	-4.77
Scaled-Max - Full DXA-driven -Max	-13.10	2.73	(-20.35, -5.84)	-4.80

Difference of Calculation Method Levels	Adjusted P-Value
DXA Scaled - Max - DXA mass driven-Max	0.000
Full DXA-driven -Max - DXA mass driven-Max	0.000
Scaled-Max - DXA mass driven-Max	0.965
Full DXA-driven -Max - DXA Scaled - Max	1.000
Scaled-Max - DXA Scaled - Max	0.000
Scaled-Max - Full DXA-driven -Max	0.000

Individual confidence level = 98.95%

Figure H.2: Repeated Measures ANOVA with Post-HOC Tukey results for Shoulder Horizontal Abduction Torque vs inverse dynamic calculation method. A Bonferroni correction factor of 4 was applied accordingly, leaving a significance level of p = 0.0125.

General Linear Model: Shoulder Compression versus ... lation Method

Method

Factor coding (-1, 0, +1)

Factor Information

Factor	Type	Levels	Values
Participants	Random	18	2017Aug20-01, 2017Aug20-02, 2017Aug20-03, 2017Jul19-01, 2017Jul19-02, 2017Jul21-01, 2017Jul21-02, 2017Jul26-01, 2017Jul27-01, 2017Jul27-02, 2017Sep07-02, 2017Sep30-01, 2018Aug01-02, 2018Aug13-01, 2018Aug15-01, 2018Aug16-01, 2018Nov07-01, 2018Nov09-02
Calculation Method	Fixed	4	DXA mass driven-Max, DXA Scaled - Max, Full DXA-driven -Max, Scaled-Max

Analysis of Variance

Source	DF	Adj SS	Adj MS	F-Value	P-Value
Participants	17	313278	18428.1	59.91	0.000
Calculation Method	3	13919	4639.7	15.08	0.000
Error	51	15688	307.6		
Total	71	342885			

Model Summary

S	R-sq	R-sq(adj)	R-sq(pred)
17.5387	95.42%	93.63%	90.88%

Coefficients

Term	Coef	SE Coef	T-Value	P-Value	VIF
Constant	-264.23	2.07	-127.84	0.000	
Participants					
2017Aug20-01	104.34	8.52	12.24	0.000	*
2017Aug20-02	73.01	8.52	8.57	0.000	*
2017Aug20-03	-41.71	8.52	-4.89	0.000	*
2017Jul19-01	51.07	8.52	5.99	0.000	*
2017Jul19-02	23.75	8.52	2.79	0.007	*
2017Jul21-01	70.48	8.52	8.27	0.000	*
2017Jul21-02	106.23	8.52	12.47	0.000	*
2017Jul26-01	-38.08	8.52	-4.47	0.000	*
2017Jul27-01	-39.86	8.52	-4.68	0.000	*
2017Jul27-02	27.94	8.52	3.28	0.002	*
2017Sep07-02	27.74	8.52	3.25	0.002	*
2017Sep30-01	-124.67	8.52	-14.63	0.000	*
2018Aug01-02	-51.10	8.52	-6.00	0.000	*
2018Aug13-01	40.42	8.52	4.74	0.000	*
2018Aug15-01	-32.38	8.52	-3.80	0.000	*
2018Aug16-01	-34.96	8.52	-4.10	0.000	*
2018Nov07-01	-57.31	8.52	-6.73	0.000	*
Calculation Method					
DXA mass driven-Max	6.51	3.58	1.82	0.075	1.50
DXA Scaled - Max	-11.87	3.58	-3.32	0.002	1.50
Full DXA-driven -Max	-14.28	3.58	-3.99	0.000	1.50

Regression Equation

Shoulder Compression = -264.23 + 104.34 Participants_2017Aug20-01
+ 73.01 Participants_2017Aug20-02 - 41.71 Participants_2017Aug20-03
+ 51.07 Participants_2017Jul19-01 + 23.75 Participants_2017Jul19-02
+ 70.48 Participants_2017Jul21-01 + 106.23 Participants_2017Jul21-02
- 38.08 Participants_2017Jul26-01 - 39.86 Participants_2017Jul27-01
+ 27.94 Participants_2017Jul27-02 + 27.74 Participants_2017Sep07-02
- 124.67 Participants_2017Sep30-01 - 51.10 Participants_2018Aug01-02
+ 40.42 Participants_2018Aug13-01 - 32.38 Participants_2018Aug15-01
- 34.96 Participants_2018Aug16-01 - 57.31 Participants_2018Nov07-01
- 104.90 Participants_2018Nov09-02 + 6.51 Calculation Method_DXA mass driven-Max - 11.87 Calculation Method_DXA Scaled - Max
- 14.28 Calculation Method_Full DXA-driven -Max
+ 19.65 Calculation Method_Scaled-Max

Equation treats random terms as though they are fixed.

Fits and Diagnostics for Unusual Observations

Obs	Shoulder Compression	Fit	Resid	Std Resid	
8	-222.67	-252.35	29.68	2.01	R
48	-435.93	-400.77	-35.15	-2.38	R
69	-301.86	-349.49	47.63	3.23	R
72	-424.69	-381.01	-43.68	-2.96	R

R Large residual

Expected Mean Squares, using Adjusted SS

	Source	Expected Mean Square for Each Term
1	Participants	(3) + 4.0000 (1)
2	Calculation Method	(3) + Q[2]
3	Error	(3)

Error Terms for Tests, using Adjusted SS

	Source	Error DF	Error MS	Synthesis of Error MS
1	Participants	51.00	307.6046	(3)
2	Calculation Method	51.00	307.6046	(3)

Variance Components, using Adjusted SS

Source	Variance	% of Total	StDev	% of Total
Participants	4530.12	93.64%	67.3062	96.77%
Error	307.605	6.36%	17.5387	25.22%
Total	4837.73		69.5538	

Comparisons for Shoulder Compression

Tukey Pairwise Comparisons: Calculation Method

Grouping Information Using the Tukey Method and 95% Confidence

Calculation Method	N	Mean	Grouping	
Scaled-Max	18	-244.582	A	
DXA mass driven-Max	18	-257.723	A	
DXA Scaled - Max	18	-276.102		B
Full DXA-driven -Max	18	-278.511		B

Means that do not share a letter are significantly different.

Tukey Simultaneous Tests for Differences of Means

Difference of Calculation Method Levels	Difference of Means	SE of Difference	Simultaneous 95% CI	T-Value
DXA Scaled - Max - DXA mass driven-Max	-18.38	5.85	(-33.92, -2.84)	-3.14
Full DXA-driven -Max - DXA mass driven-Max	-20.79	5.85	(-36.33, -5.24)	-3.56
Scaled-Max - DXA mass driven-Max	13.14	5.85	(-2.40, 28.68)	2.25
Full DXA-driven -Max - DXA Scaled - Max	-2.41	5.85	(-17.95, 13.13)	-0.41
Scaled-Max - DXA Scaled - Max	31.52	5.85	(15.98, 47.06)	5.39
Scaled-Max - Full DXA-driven -Max	33.93	5.85	(18.39, 49.47)	5.80

Difference of Calculation Method Levels	Adjusted P-Value
DXA Scaled - Max - DXA mass driven-Max	0.014
Full DXA-driven -Max - DXA mass driven-Max	0.004
Scaled-Max - DXA mass driven-Max	0.124
Full DXA-driven -Max - DXA Scaled - Max	0.976
Scaled-Max - DXA Scaled - Max	0.000
Scaled-Max - Full DXA-driven -Max	0.000

Individual confidence level = 98.95%

Figure H.3: Repeated Measures ANOVA with Post-HOC Tukey results for Shoulder Compression Force vs inverse dynamic calculation method. A Bonferroni correction factor of 4 was applied accordingly, leaving a significance level of p = 0.0125.

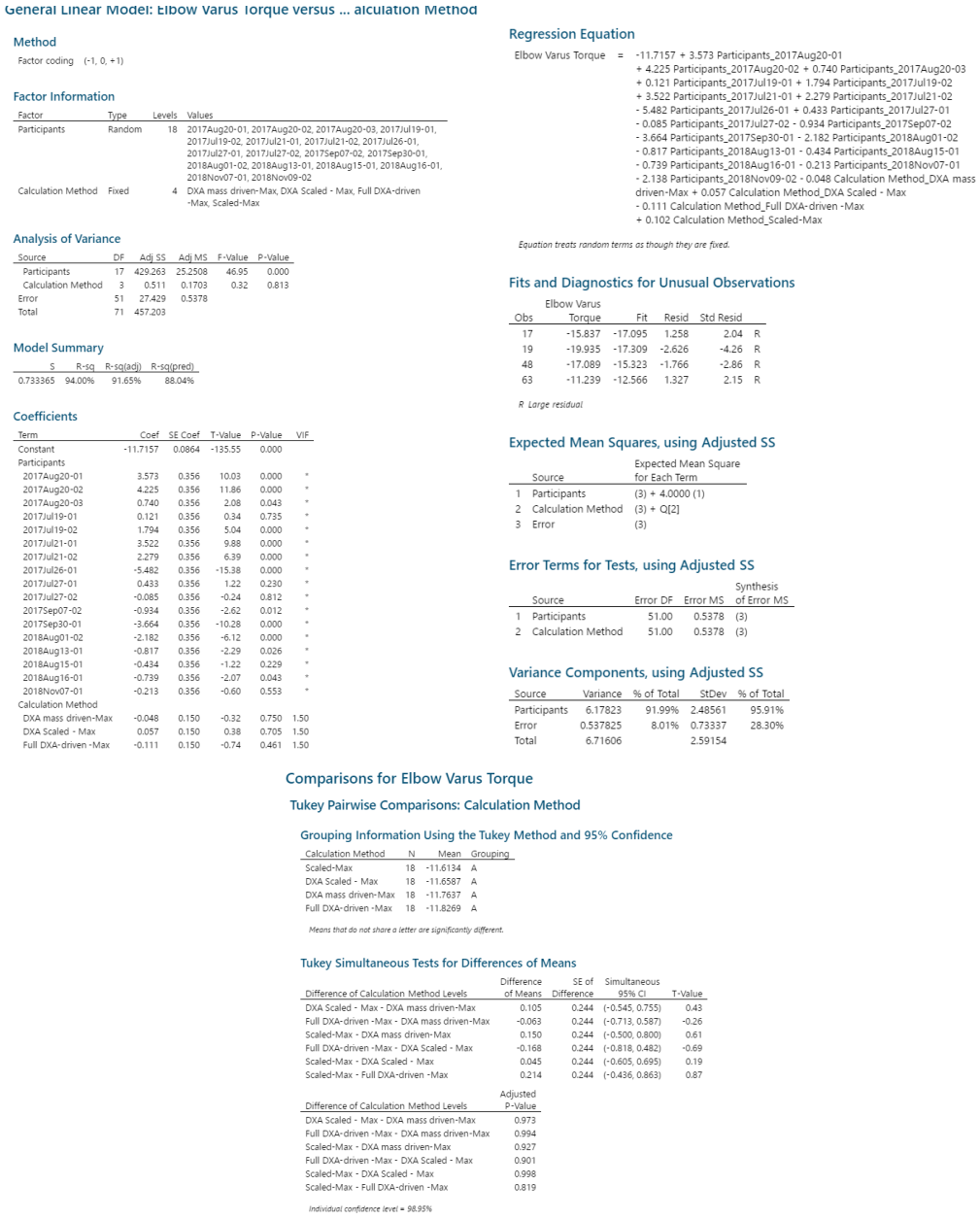

General Linear Model: Elbow Varus Torque versus ... alculation Method

Method

Factor coding (-1, 0, +1)

Factor Information

Factor	Type	Levels	Values
Participants	Random	18	2017Aug20-01, 2017Aug20-02, 2017Aug20-03, 2017Jul19-01, 2017Jul19-02, 2017Jul21-01, 2017Jul21-02, 2017Jul26-01, 2017Jul27-01, 2017Jul27-02, 2017Sep07-02, 2017Sep30-01, 2018Aug01-02, 2018Aug13-01, 2018Aug15-01, 2018Aug16-01, 2018Nov07-01, 2018Nov09-02
Calculation Method	Fixed	4	DXA mass driven-Max, DXA Scaled - Max, Full DXA-driven -Max, Scaled-Max

Analysis of Variance

Source	DF	Adj SS	Adj MS	F-Value	P-Value
Participants	17	429.263	25.2508	46.95	0.000
Calculation Method	3	0.511	0.1703	0.32	0.813
Error	51	27.429	0.5378		
Total	71	457.203			

Model Summary

S	R-sq	R-sq(adj)	R-sq(pred)
0.733365	94.00%	91.65%	88.04%

Coefficients

Term	Coef	SE Coef	T-Value	P-Value	VIF
Constant	-11.7157	0.0864	-135.55	0.000	
Participants					
2017Aug20-01	3.573	0.356	10.03	0.000	*
2017Aug20-02	4.225	0.356	11.86	0.000	*
2017Aug20-03	0.740	0.356	2.08	0.043	*
2017Jul19-01	0.121	0.356	0.34	0.735	*
2017Jul19-02	1.794	0.356	5.04	0.000	*
2017Jul21-01	3.522	0.356	9.88	0.000	*
2017Jul21-02	2.279	0.356	6.39	0.000	*
2017Jul26-01	-5.482	0.356	-15.38	0.000	*
2017Jul27-01	0.433	0.356	1.22	0.230	*
2017Jul27-02	-0.085	0.356	-0.24	0.812	*
2017Sep07-02	-0.934	0.356	-2.62	0.012	*
2017Sep30-01	-3.664	0.356	-10.28	0.000	*
2018Aug01-02	-2.182	0.356	-6.12	0.000	*
2018Aug13-01	-0.817	0.356	-2.29	0.026	*
2018Aug15-01	-0.434	0.356	-1.22	0.229	*
2018Aug16-01	-0.739	0.356	-2.07	0.043	*
2018Nov07-01	-0.213	0.356	-0.60	0.553	*
Calculation Method					
DXA mass driven-Max	-0.048	0.150	-0.32	0.750	1.50
DXA Scaled - Max	0.057	0.150	0.38	0.705	1.50
Full DXA-driven -Max	-0.111	0.150	-0.74	0.461	1.50

Regression Equation

Elbow Varus Torque = -11.7157 + 3.573 Participants_2017Aug20-01
+ 4.225 Participants_2017Aug20-02 + 0.740 Participants_2017Aug20-03
+ 0.121 Participants_2017Jul19-01 + 1.794 Participants_2017Jul19-02
+ 3.522 Participants_2017Jul21-01 + 2.279 Participants_2017Jul21-02
- 5.482 Participants_2017Jul26-01 + 0.433 Participants_2017Jul27-01
- 0.085 Participants_2017Jul27-02 - 0.934 Participants_2017Sep07-02
- 3.664 Participants_2017Sep30-01 - 2.182 Participants_2018Aug01-02
- 0.817 Participants_2018Aug13-01 - 0.434 Participants_2018Aug15-01
- 0.739 Participants_2018Aug16-01 - 0.213 Participants_2018Nov07-01
- 2.138 Participants_2018Nov09-02 - 0.048 Calculation Method_DXA mass driven-Max + 0.057 Calculation Method_DXA Scaled - Max
- 0.111 Calculation Method_Full DXA-driven -Max
+ 0.102 Calculation Method_Scaled-Max

Equation treats random terms as though they are fixed.

Fits and Diagnostics for Unusual Observations

Obs	Elbow Varus Torque	Fit	Resid	Std Resid	
17	-15.837	-17.095	1.258	2.04	R
19	-19.935	-17.309	-2.626	-4.26	R
48	-17.089	-15.323	-1.766	-2.86	R
63	-11.239	-12.566	1.327	2.15	R

R Large residual

Expected Mean Squares, using Adjusted SS

	Source	Expected Mean Square for Each Term
1	Participants	(3) + 4.0000 (1)
2	Calculation Method	(3) + Q[2]
3	Error	(3)

Error Terms for Tests, using Adjusted SS

	Source	Error DF	Error MS	Synthesis of Error MS
1	Participants	51.00	0.5378	(3)
2	Calculation Method	51.00	0.5378	(3)

Variance Components, using Adjusted SS

Source	Variance	% of Total	StDev	% of Total
Participants	6.17823	91.99%	2.48561	95.91%
Error	0.537825	8.01%	0.73337	28.30%
Total	6.71606		2.59154	

Comparisons for Elbow Varus Torque

Tukey Pairwise Comparisons: Calculation Method

Grouping Information Using the Tukey Method and 95% Confidence

Calculation Method	N	Mean	Grouping
Scaled-Max	18	-11.6134	A
DXA Scaled - Max	18	-11.6587	A
DXA mass driven-Max	18	-11.7637	A
Full DXA-driven -Max	18	-11.8269	A

Means that do not share a letter are significantly different.

Tukey Simultaneous Tests for Differences of Means

Difference of Calculation Method Levels	Difference of Means	SE of Difference	Simultaneous 95% CI	T-Value
DXA Scaled - Max - DXA mass driven-Max	0.105	0.244	(-0.545, 0.755)	0.43
Full DXA-driven -Max - DXA mass driven-Max	-0.063	0.244	(-0.713, 0.587)	-0.26
Scaled-Max - DXA mass driven-Max	0.150	0.244	(-0.500, 0.800)	0.61
Full DXA-driven -Max - DXA Scaled - Max	-0.168	0.244	(-0.818, 0.482)	-0.69
Scaled-Max - DXA Scaled - Max	0.045	0.244	(-0.605, 0.695)	0.19
Scaled-Max - Full DXA-driven -Max	0.214	0.244	(-0.436, 0.863)	0.87

Difference of Calculation Method Levels	Adjusted P-Value
DXA Scaled - Max - DXA mass driven-Max	0.973
Full DXA-driven -Max - DXA mass driven-Max	0.994
Scaled-Max - DXA mass driven-Max	0.927
Full DXA-driven -Max - DXA Scaled - Max	0.901
Scaled-Max - DXA Scaled - Max	0.998
Scaled-Max - Full DXA-driven -Max	0.819

Individual confidence level = 98.95%

Figure H.4: Repeated Measures ANOVA with Post-HOC Tukey results for Elbow Varus Torque vs inverse dynamic calculation method. A Bonferroni correction factor of 4 was applied accordingly, leaving a significance level of p = 0.0125.